NSG-3017

COLLEGE OF ENGINEERING

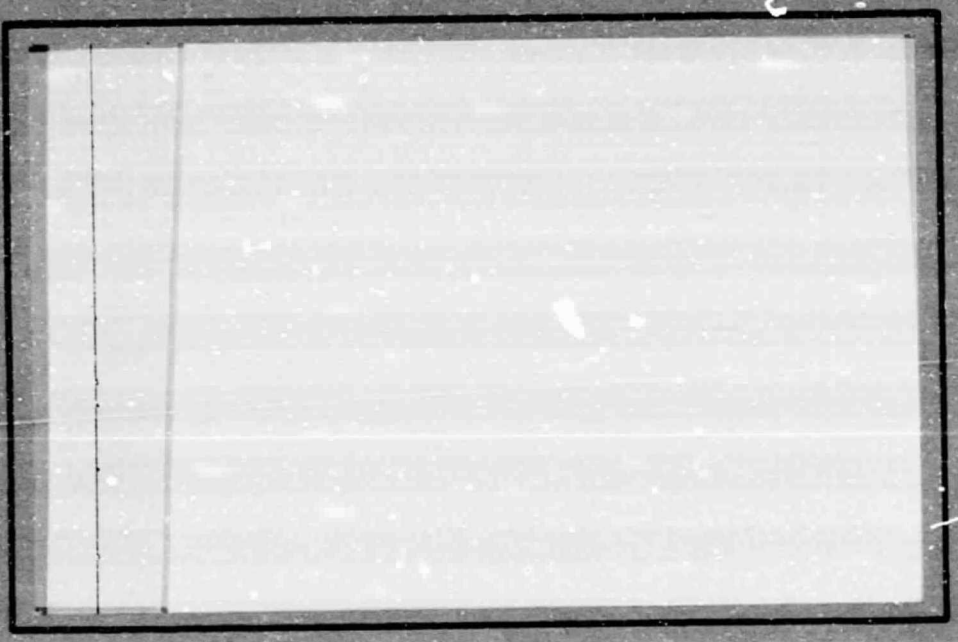

VIRGINIA POLYTECHNIC INSTITUTE AND STATE UNIVERSITY

BLACKSBURG, VIRGINIA

AN INVESTIGATION OF AEROELASTIC PHENOMENA ASSOCIATED WITH AN OBLIQUE WINGED AIRCRAFT

Final Technical Report
NASA/Ames Research Center
Grant NSG-2016
31 August 1976

Dr. Terry A. Weisshaar*
Principal Investigator

*Assistant Professor, Aerospace and Ocean Engineering Department, Virginia Polytechnic Institute and State University, Blacksburg, Virginia 24061.

PURPOSE

This report describes the results of research sponsored under NASA/Ames Research Center Grant NSG-2016 from 1 April 1974 through 31 August 1976. Principal investigator for this grant was Dr. Terry A. Weisshaar, Assistant Professor, Aerospace and Ocean Engineering Department, Virginia Polytechnic Institute and State University, Blacksburg, Virginia. The grant monitor was Mr. Peter A. Gaspers, Aeronautical Structures Branch, NASA/Ames Research Center, Mofíett Field, California.

TABLE OF CONTENTS

	Page
Introduction	1
Static Aeroelastic Characteristics	1
Subsonic Flutter Studies	4
Supersonic Flutter Behavior	8
Wing Tailoring	11
Conclusions	13
References	14
Figures	16

INTRODUCTION

The reappearance of the oblique winged aircraft concept, as recently proposed by R. T. Jones of NASA/Ames Research Center, has led to the need for serious study of questions related to the aeroelastic behavior of such aircraft. This report reviews the oblique wing aeroelasticity studies conducted at Virginia Polytechnic Institute and State University. These studies had two objectives; first of all, the static aeroelastic stability characteristics of oblique wing aircraft were examined, together with lateral trim requirements for 1-g flight. In addition, the dynamic aeroelastic stability behavior of oblique winged aircraft, primarily flutter, was assessed. From these studies has emerged a better understanding of the similarities and differences between oblique winged aircraft and conventional, bilaterally symmetric, swept wing aircraft.

STATIC AEROELASTIC CHARACTERISTICS

Because the proposed oblique wing aircraft uses an asymmetrically swept wing (Fig. 1), there exists an undesirable tendency of the aircraft to roll in the absence of lateral control. Two cases must be considered to study this tendency; these cases concern a hypothetical rigid wing aircraft and the more realistic, flexible wing aircraft.

Consider first an oblique wing which will not deform under an applied load. As the aircraft flies at progressively higher speeds, an examination of the spanwise pressure distribution reveals that lift tends to "build-up" towards the downstream wing tip. The span-wise lift distribution thus appears skewed toward the side with the sweptback

wing. This unsymmetrical pressure distribution introduces a roll moment. This roll moment tends to elevate the sweptback wing and therefore must be countered either by deflection of control surfaces or by an initial, built-in twist distribution.

A flexible wing behaves somewhat differently. It is well-known that when a moderately sweptback wing deforms, the induced angle of attack at each spanwise station is decreased. Thus, the center of lift for the wing moves inboard and forward. The converse is true for flexible swept-forward wings where, under an upward load, the spanwise center of lift is shifted outboard and forward. This behavior of symmetrically swept flexible wings accounts for the fact that sweptback wings tend to attenuate changes in lift due to gusts while sweptforward wings tend to amplify these changes.

A flexible, obliquely-swept wing will tend to develop more lift on the sweptforward surface than on the sweptback surface. This unequal lift distribution will cause the sweptforward wing to rise, exactly the opposite tendency seen for a rigid wing. The amount of aeroelastic roll moment present is a function of the airstream dynamic pressure and the wing geometry and material properties.

Several studies were conducted to assess the importance of static aeroelastic effects to the design of oblique wing aircraft. These studies primarily involved assessments of aileron effectiveness in maintaining lateral trim and the amount of trim necessary at various flight speeds.

Reference 1 describes a study of the effectiveness of ailerons when used to control lateral oscillations of a flexible oblique wing aircraft. This study found that there was, in fact, an aileron reversal speed

associated with this type of aircraft; this speed was found to be fairly large. This finding was significant because a bilaterally symmetric sweptforward wing usually does not have a reversal speed associated with it, while a bilaterally symmetric sweptback wing may have a relatively low aileron reversal speed. Reference 1 also determined that the oblique wing aircraft did not encounter a static aeroelastic divergence condition when using ailerons to damp out lateral oscillations. It was also determined that the ratio of wing-to-fuselage mass moments of inertia plays an important role in the dynamic stability behavior of oblique wing aircraft.

Reference 2 explores the aeroelastically induced roll moment in a preliminary fashion. The significant finding of this paper is that the roll moment on a clamped oblique wing was shown to rise rapidly with dynamic pressure. In addition, once ailerons are applied to achieve lateral equilibrium, the wing root bending moment on the sweptforward wing is magnified considerably by aeroelastic effects. The fact that the model considered in Ref. 2 was not subject to a constant lift restriction makes the application of the results to an actual aircraft difficult.

Reference 3 studies the more realistic problem of achieving lateral equilibrium while maintaining level or 1-g flight. Among the results of this analysis were that aileron trim settings of a few degrees are sufficient to trim an oblique wing aircraft in roll for level 1-g flight. Also, the use of socalled built-in twist in the form of an initial wing anhedral may be used to ensure lateral trim equilibrium.

The theoretical planform model used for these latter studies is shown in Fig. 2. Figure 3 shows the amount of initial anhedral ψ_o (in degrees) needed per unit of wing loading (W/s lb/ft.^{2}) necessary to

maintain lateral trim of a wind-tunnel flexible model. Results shown are the results of using both aerodynamic strip theory and a more accurate aerodynamic model. Also of interest is the fact that, when the aircraft is trimmed in roll, the proportion of the total lift carried by each wing is different. Fig. 4 illustrates a strip theory prediction of these fractions as a function of the nondimensional variable q^*. This variable q^* expresses the ratio of the aircraft operating dynamic pressure, q, to the dynamic pressure, q_{DIV}, at which a clamped oblique wing is found to diverge aeroelastically. It is seen that, as this ratio increases, the sweptback wing begins to carry more of the total load than does the swept-forward wing. However, as the sweptback wing "loads up", its center of pressure moves inboard. This simultaneous action produces the somewhat remarkable result that the bending moment at the wing root varies little with q^*.

Reference 4 describes a computer program developed at V.P.I. for NASA/Ames Research Center to analyze lateral trim requirements. This program uses elementary beam theory together with an accurate aerodynamic model to analyze nonuniform planform wings. This program was successfully used to support additional NASA oblique wing studies.

SUBSONIC FLUTTER STUDIES

Of particular importance is the aeroelastic stability behavior of oblique wing aircraft. The concern about aeroelastic stability arises primarily because of the well-known tendency of bilaterally symmetric sweptforward wings to have relatively low divergence speeds; it is this

by computation of the spanwise static airload distribution and subsequent determination of stresses.

Of particular interest are the tapered wing studies in Ref. 6. Figure 6 shows planform layouts for four semi-spans studied. Of these semi-spans, the one with a taper ratio (TR) of 0.50 most closely approximates that found on actual transport wings. Figure 7 illustrates the effects of the inclusion of the various rigid body degrees of freedom into the flutter analysis. From this figure, it is seen that the inclusion of roll freedom into the problem is the most significant of the three rigid body freedoms considered.

Figure 8 illustrates the effect of placing the chordwise center of mass position at various points on the wing. Since the line of aerodynamic centers is near the one-quarter chord, aft positions are unfavorable to the flutter performance of the wing. This importance of center of mass position is diminished with increasing sweep angle.

An additional interesting result presented in Ref. 6 is illustrated in Figures 9, 10 and 11. These figures show V-g stability plots; these plots indicate that, for this particular configuration, the body-freedom mode of instability does not occur at all until a sweep angle of 60 degrees is reached. Unfortunately, the reasons for this behavior were not ascertained.

SUPERSONIC FLUTTER BEHAVIOR

Because, from a lift-to-drag standpoint, the oblique wing aircraft encounters its most favorable flight conditions in the supersonic flight

characteristic which leads to large weight penalties because of the need for additional stiffening. Divergence is a quasi-static phenomenon involving an unstable aperiodic deformation of the wing. For purposes of analysis, the wing behavior can be treated as being static, with the result that mass properties of the aircraft are not necessary for the determination of the instability.

The characteristic which makes the oblique wing behave differently than the symmetrical sweptforward wing is that the oblique wing tends to roll if it undergoes symmetrical deformations. The symmetrical sweptforward wing is free to develop large symmetrical static deformations under the action of the airstream without developing a roll moment while an oblique wing free to roll cannot do so without introducing a roll moment. This roll moment causes angular acceleration, which in turn introduces significant inertia loads into the problem. Therefore, any aeroelastic stability analysis of oblique wing aircraft of necessity must be a dynamic analysis.

A preliminary study by the Boeing Company presented by Jones and Nisbet (Ref. 5) indicated that the mode of oblique wing aeroelastic instability was flutter; this flutter speed was found to occur at a slightly higher speed than the divergence speed found for a similar oblique wing with clamped root condition. Thus, the introduction of the rigid-body-roll degree of freedom was found to stabilize the oblique wing system.

The flutter study described in Ref. 5 was limited in scope; further investigations were necessary to determine the effect of the myriad of parameters involved in wing flutter determination. To accomplish this, a computer program was developed at V.P.I. to analyze the flutter behavior

of swept wings in the subsonic flight regime. This program, together with many flutter studies using this program, is described in Ref. 6.

The computer program described above was first used to study the aeroelastic stability behavior of a few small, flexible, wind-tunnel models (Ref. 7, 8). These analyses further confirmed the importance of the rigid-body roll freedom to the aeroelastic stability of oblique wing aircraft. Figure 5 shows a typical stability curve where a nondimensional flutter velocity is plotted against the oblique sweep angle, Λ. The model used consisted of a nearly elliptical wing planform constructed of thin-sheet aluminum. The parameter V_{DO} represents the calculated divergence speed of the oblique wing, in its unswept position, when it is not free to roll. Figure 5 clearly shows the decline in divergence speed as sweep angle increases.

When the wing is given freedom to roll, the divergence instability mode changes from divergence to flutter. With the wing free to roll, two types of flutter instability are observed to occur. One type of instability involves an oscillatory mode with coupled bending-torsion deformation, but with very little rigid-body roll motion present. The reduced frequency, k, ($k = \omega b/V$ where ω = oscillation frequency in radians/sec.; b = semi-chord parallel to the flow; V = air velocity) at the onset of flutter is found to be relatively high, $k \tilde{=} 0.30$. This type of flutter instability has the characteristic that the flutter speed increases with increasing Λ. Because very little roll coupling is present in this type of instability, it is termed "fixed-root" flutter.

A second type of flutter instability for the roll free aircraft is found to occur. This instability involves an oscillatory motion in which

bending-torsion oscillations are strongly coupled with a substantial amount of rigid-body roll motion. This type of instability is termed "body-freedom" flutter. Associated with body-freedom flutter are relatively small values of reduced frequency, k, of the order of $k \tilde{=} 0.03$. Body freedom flutter speeds are seen to decline with increasing values of Λ.

For small to moderate values of sweep angle, the fixed-root type of flutter will occur at lower speeds than body-freedom flutter. The reverse is true at larger sweep angles. The changeover from one type of flutter instability to the other is marked by a cusp in the stability curve. Referring to Fig. 5, it is seen that this cusp appears at higher values of Λ as the fuselage mass moment of inertia, I_f, decreases relative to the wing mass moment of inertia (in the unswept position), I_0. The inclusion of freedom to roll may greatly increase the aeroelastic instability speed, depending upon the sweep angle. It should be noted that very little increase in flutter speed is found at large sweep angles.

As was previously mentioned, Reference 6 presents a wealth of information on oblique wing flutter in incompressible flow and in compressible subsonic flow. The studies presented in Ref. 6 were conducted using a finite element structural analysis method together with the Doublet-Lattice method for unsteady aerodynamic force computation.

Unlike the studies in Refs. 7,8, Ref. 6 concerns itself with full-scale, transport category aircraft. Wing sizing to determine the spanwise inertia and stiffness distributions was accomplished by developing wing inertia characteristics similar to those of existing aircraft wings and

regime, a study was conducted to determine its flutter behavior in this flight regime. In the early stages of this study, it was found that existing programmed computational methods suitable for generating aerodynamic influence coefficients were restricted to bilaterally symmetric wing planforms. Because of the amount of time and expense involved in programming the computation of an accurate 3-D aerodynamic influence coefficient generator, a simple but meaningful approach was substituted.

Reference 9 presents a study of the supersonic flutter behavior of an oblique wing model. This model consists of a rectangular wing planform with a rigid-body roll degree of freedom. A quasi-steady, linearized, two-dimensional aerodynamic theory was used to model the aerodynamic forces acting on this model. Parameters examined for the study include aspect ratio, Mach number, fundamental bending-torsion frequency ratio and wing-fuselage roll mass moment of inertia ratio.

Figure 12 illustrates the effect on flutter of the wing-to-fuselage roll mass moment of inertia ratio. From this figure, it may be determined that the effect of this ratio is similar to that seen at subsonic speeds.

Figure 13 shows the influence of wing aspect ratio on the flutter behavior of oblique wings. An examination of this figure reveals that increasing aspect ratio is destabilizing when fixed-root flutter occurs, but is stabilizing when body-freedom flutter occurs. Figure 14 illustrates the importance of the position of the wing elastic axis (E.A.) with respect to the mid-chord line. Because the aerodynamic theory used in the study places the wing aerodynamic center at the mid-chord, an E.A. ahead of the mid-chord is favorable for flutter because upward lift forces tend to impart

a downward twist to the wing and thus at least partially decrease the flexible angle of attack. The converse is true for E.A. positions aft of the mid-chord line. Also to be noted is the fact that E. A. position is more important at low sweep angles, where fixed-root flutter occurs, than at moderate to large sweep angles where body-freedom flutter predominates.

Bending-torsion frequency ratio is also seen to be an important parameter in the determination of oblique wing flutter; Figure 15 illustrates this importance. If the torsional stiffness, which is due mainly to the presence of the wing's metal skin, is held constant while the bending stiffness is increased, two effects occur. For frequency ratio values less than unity, the fixed root flutter speeds decrease, while body-freedom flutter speeds increase. At some point, the flutter behavior becomes entirely that of the fixed-root type, in the range of practical interest. As the frequency ratio is increased from unity, the fixed-root flutter speeds again increase, while the body-freedom flutter mode still remains absent. The stiffening of the wing in bending appears beneficial only for moderate to large sweep angles.

Figure 16 shows the influence of Mach number on oblique wing flutter. The stiffness - altitude parameter $\beta = (b\omega_\theta/a_\infty)\sqrt{\mu}$ is plotted against the sweep angle Λ. In this case ω_θ is the fundamental clamped torsional natural frequency of the wing while a_∞ = speed of sound and μ is a relative density parameter related to the airstream density and the density of the wing. From this figure it is determined that higher operating Mach numbers will require combinations of parameters such as higher torsional stiffness (and bending stiffness) with the associated increase in weight,

lower speeds of sound (associated with higher altitude) or larger mass ratios, attributable either to decreased air density or higher wing density.

WING TAILORING

One study, described in Ref. 10, was conducted to determine the optimal or least-weight distribution of structural material in the wing for a given static divergence speed. This study was similar to a study (Ref. 11) done at NASA/Ames by Gwin in 1974. Although the objectives of Ref. 10 were modest, several interesting results of that study are worthy of mention.

Ref. 10 describes a search for a least-weight design of an oblique wing, clamped at the root, subject to two behavioral constraints. These constraints are that the divergence speed be fixed and that the flight loads encountered during one-g flight be carried by the wing with adequate safety margins. No lateral trim requirements were imposed for this study. However, the imposition of statically indeterminate load constraint relations represents an improvement over Ref. 11. In addition, no elastic wing symmetry requirements were imposed on the aircraft.

Figure 17 gives an indication of the optimal amount of bending material necessary for divergence only and for strength only constraints. From this figure it is seen that, for symmetrical swept wing aircraft, the divergence constraint imposes a much more severe weight penalty than does the strength-only constraint. The increase in weight necessary when the wings are symmetrically swept forward stems from the outward movement of the spanwise

center of pressure caused by aeroelastic deformation. Also to be noted is that divergence is not really a consideration for symmetrical sweptback wings.

An additional interesting comparison contained in Ref. 10 concerns the error introduced if aeroelastic effects on spanwise loading are neglected. If the wing is assumed to be rigid, then the computation of wing stresses from simple beam theory involves a statically determinate problem. If the wing is flexible, however, the problem loads are deflection dependent; so too are the internal stresses. Figure 18 illustrates the effect of disregarding flexibility on a strength-constrained unswept wing. The flexible wing is more substantial than the rigid wing because of the outward spanwise movement of the wing center of pressure. Figures 19 and 20 illustrate the importance of flexibility on the minimum weight design. A 15 degree sweptback wing design shows little sensitivity to flexibility for the constraint imposed. However, the sweptforward wing is seen to be very sensitive to flexibility effects.

Figures 21, 22, 23 and 24 illustrate optimal distributions of bending material for a clamped oblique wing with constant one-g lift at various oblique sweep angles. The effect of the divergence constraint on the sweptforward wing is clearly seen in these figures. With the wing clamped and with no roll control applied, the strength constraint has a different meaning than is the case on a roll-free aircraft. However, these results use, for comparison purposes, the same constraints used in Ref. 11. The results of Ref. 10 indicate that anti-symmetrical optimal elastic tailoring produces semi-spans with greatly differing stiffness distributions. In

addition, strength appears to be the governing criteria for the sweptback portion of the wing while divergence governs the sweptforward wing design. Finally, Fig. 25 presents least weight objective function values for several oblique sweep angles.

CONCLUSIONS

From the voluminous studies completed during the past two years several important conclusions may be drawn.

(a) The mode of instability for oblique winged aircraft is flutter. This result stems from the fact that the fuselage is roll-free.

(b) Two basic types of flutter are found to occur; these are body-freedom flutter and fixed-root flutter. Generalizations about fixed-root flutter behavior seem to be similar to those applicable for symmetrical aircraft. On the other hand, body-freedom flutter, while a dynamic instability, seems to be governed by most of the same general rules that apply to symmetrical sweptforward wing divergence.

(c) One method of preventing body-freedom flutter, stiffening the wing in bending, results in large weight penalties. Other means of controlling the flutter mode and speed are available which may not involve such severe penalties. These methods include using large aspect ratio wings with slender fuselages or tailoring bending-torsion stiffness ratios to achieve better performance.

(d) The basic character of the flutter behavior of oblique wing aircraft in the subsonic flight regime is the same as in the supersonic flight regime.

REFERENCES

1. Weisshaar, T. A. and Ashley, H., "Static Aeroelasticity and the Flying Wing-Revisited," AIAA Journal of Aircraft, Vol. 11, No. 11, November 1974, pp. 718-720.
2. Weisshaar, T. A., Influence of Static Aeroelasticity on Oblique Winged Aircraft," AIAA Journal of Aircraft, Vol. 11, No. 4, April 1974, pp. 247-249.
3. Weisshaar, T. A., "Lateral Equilibrium of Asymmetrically Swept Wings-Aileron Control vs. Geometric Twist," (To appear in the AIAA Journal of Aircraft).
4. Weisshaar, T. A., "The AIRLOD Computer Code-Static Aeroelastic Characteristics of Oblique Swept Wings," Virginia Polytechnic Institute and State University, Blacksburg, Virginia, 1975.
5. Jones, R. T. and Nisbet, J. W., "Transonic Transport Wings - Oblique or Swept," Astronautics and Aeronautics, Vol. 12, No. 1, January 1974, pp. 40-47.
6. Crittenden, J. B., "Aeroelastic Stability Behavior of Oblique-Winged Aircraft," Ph.D. Thesis, Aerospace and Ocean Engineering Dept., Virginia Polytechnic Institute and State University, Blacksburg, Virginia, February, 1976.
7. Weisshaar, T. A. and Crittenden, J. B., "Flutter of Asymmetrically Swept Wings," (to appear in the AIAA Journal).
8. Weisshaar, T. A. and Crittenden, J. B., "Flutter of Asymmetrically Swept Wings," Report No. 55, Aerospace and Ocean Engineering Department, Virginia Polytechnic Institute and State University, Blacksburg, Virginia, August 1976.

9. Weisshaar, T. A., "Supersonic Flutter of Asymmetrically Swept Wings," Report No. 56, Aerospace and Ocean Engineering Department, Virginia Polytechnic Institute and State University, Blacksburg, Virginia, August 1976.

10. Kudva, N. J., "Structural Optimization of Oblique and Symmetrical Swept Wing Aircraft," M. S. Thesis, Aerospace and Ocean Engineering Department, Virginia Polytechnic Institute and State University, Blacksburg, Virginia, May 1976.

11. Gwin, L. B., "Optimal Aeroelastic Design of an Oblique Wing Structure," AIAA Paper No. 74-349, April, 1974.

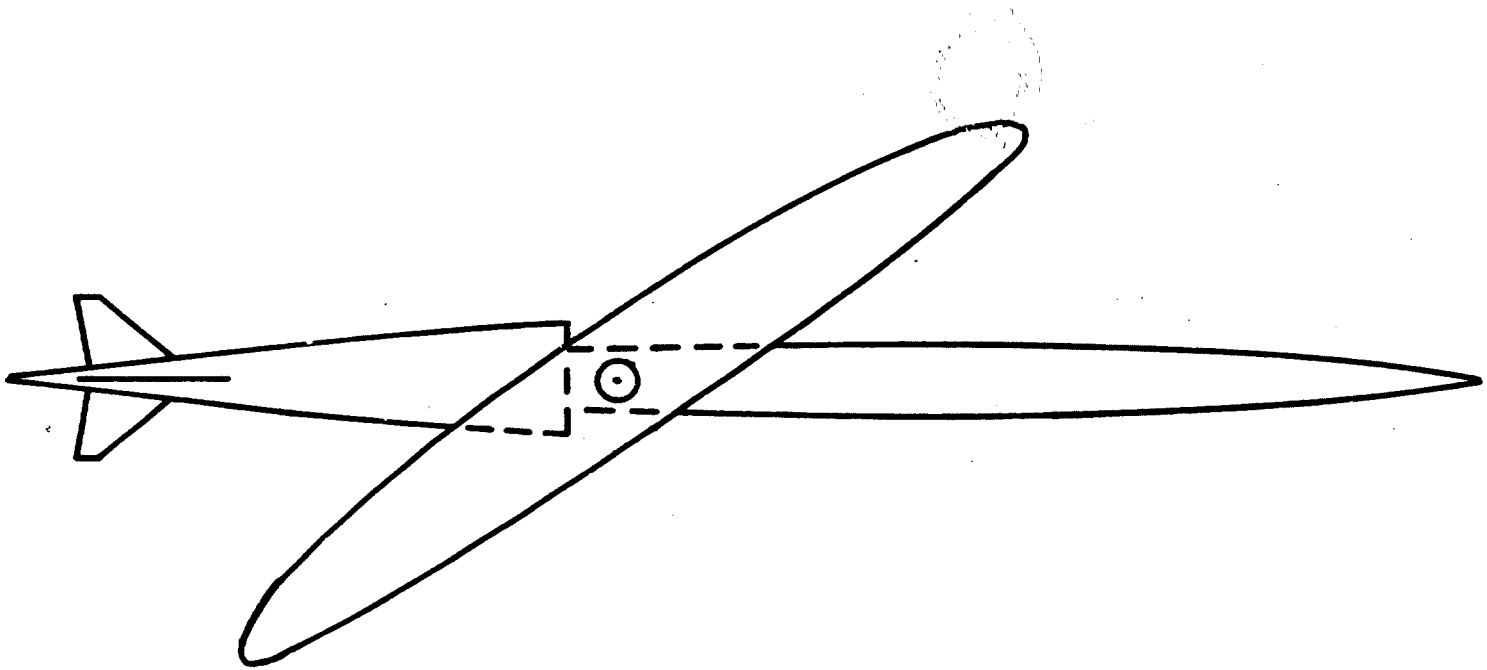

Fig. 1 - Oblique-Winged Aircraft Planform

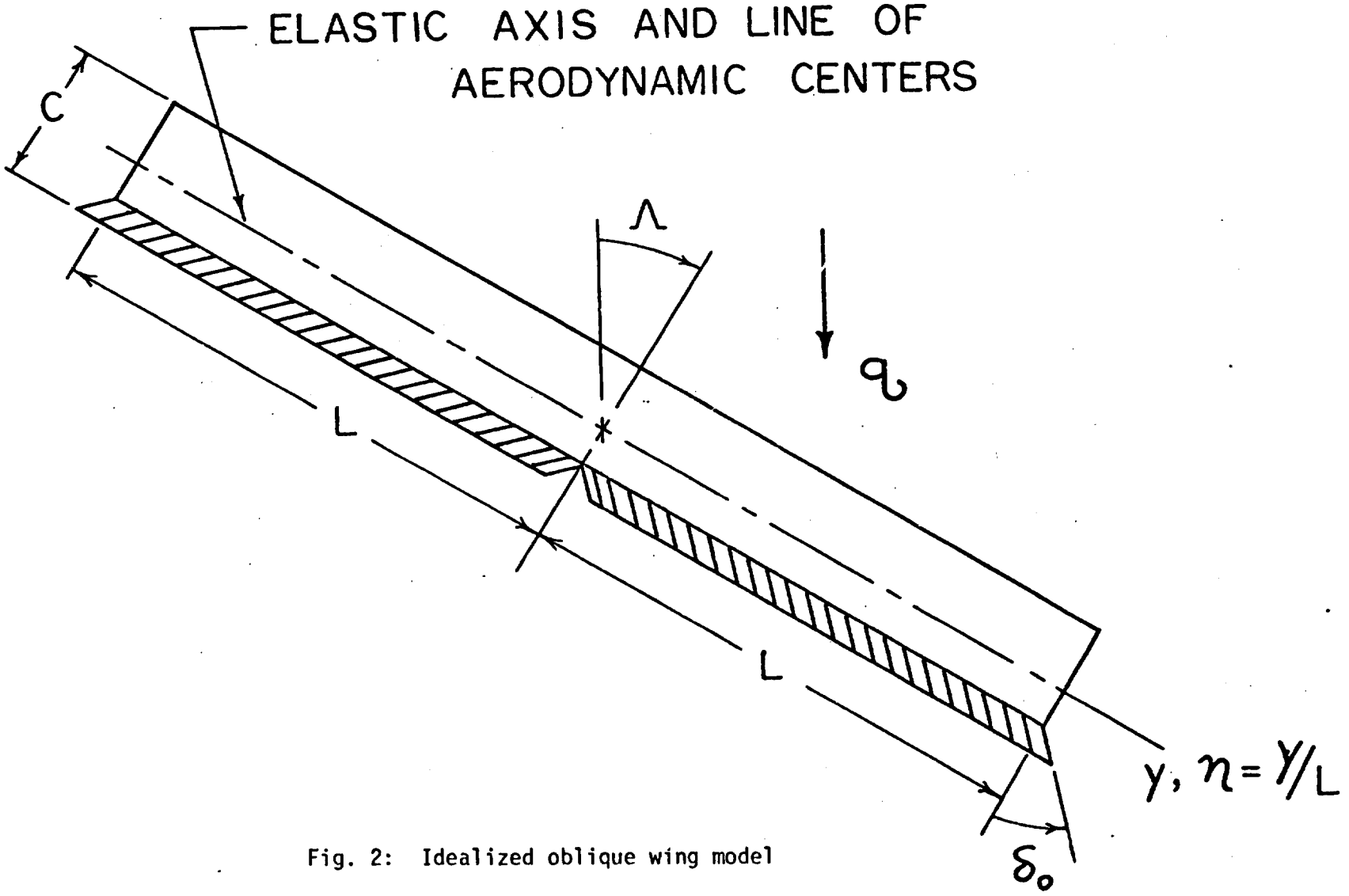

Fig. 2: Idealized oblique wing model

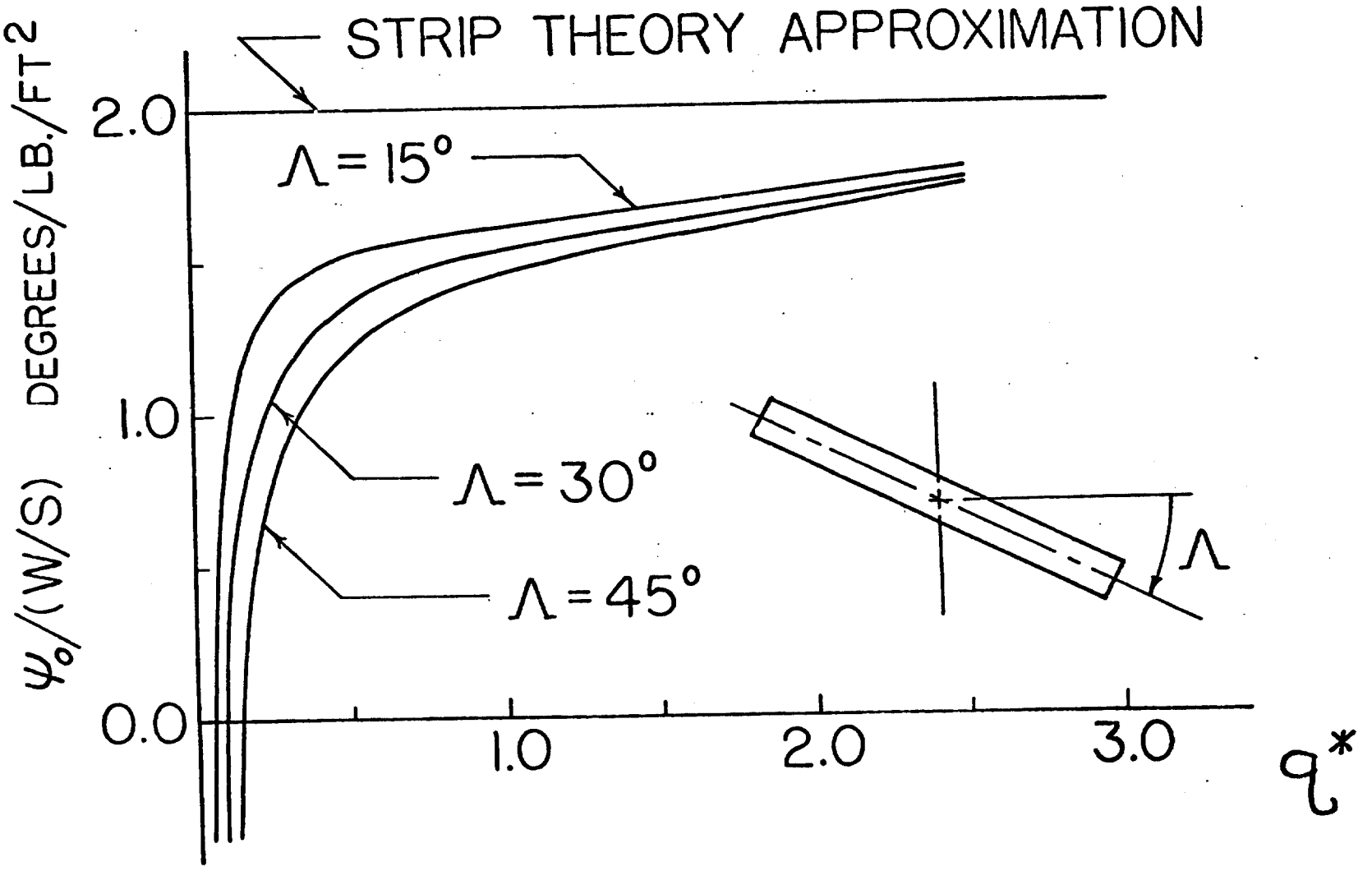

Fig. 3: Required wing anhedral vs. pressure parameter for several sweep angles. (Ref. 3)

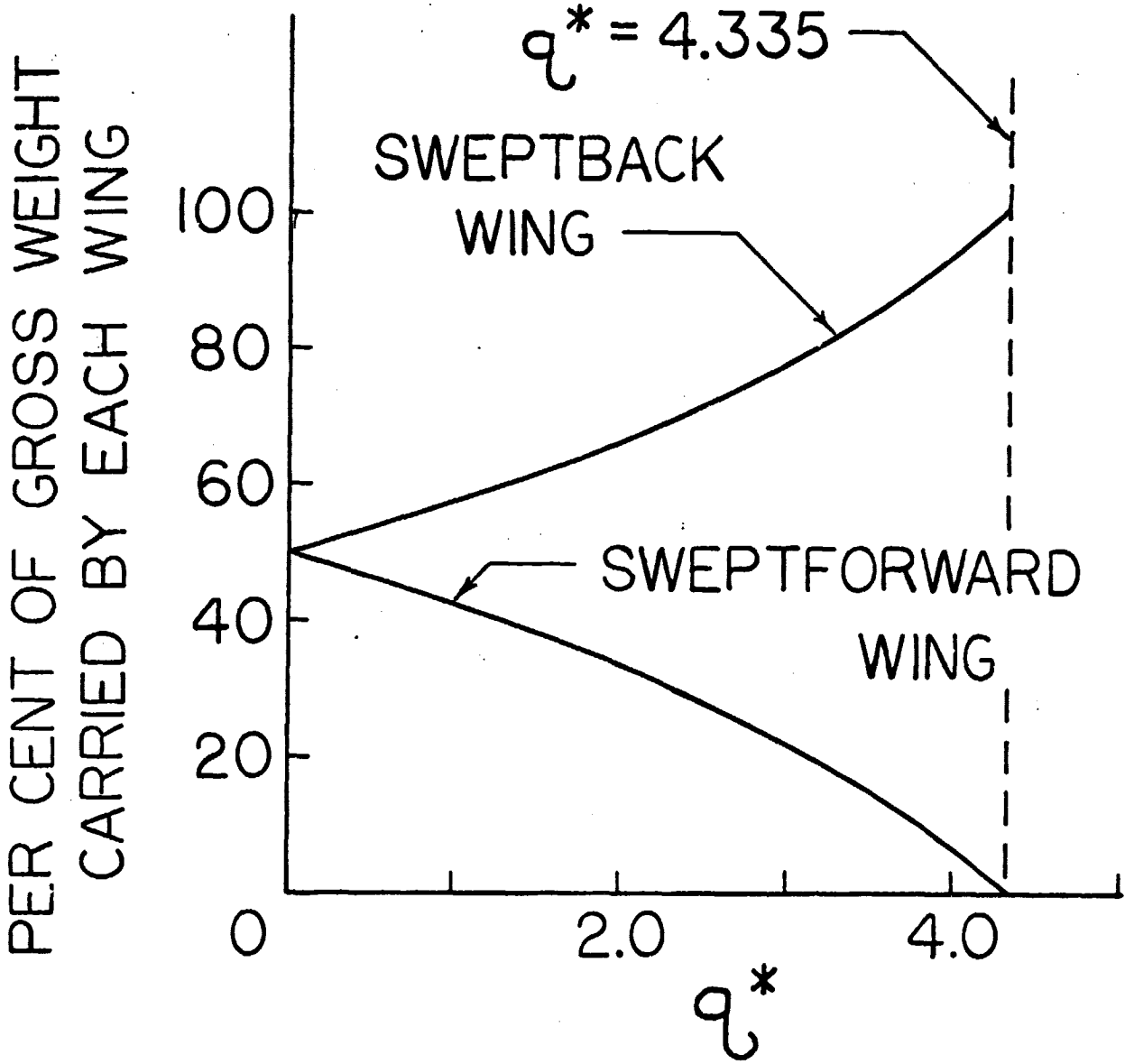

Fig. 4: Strip theory prediction of percentage of total weight carried by each oblique wing semi-span vs. pressure parameter. (Ref. 3).

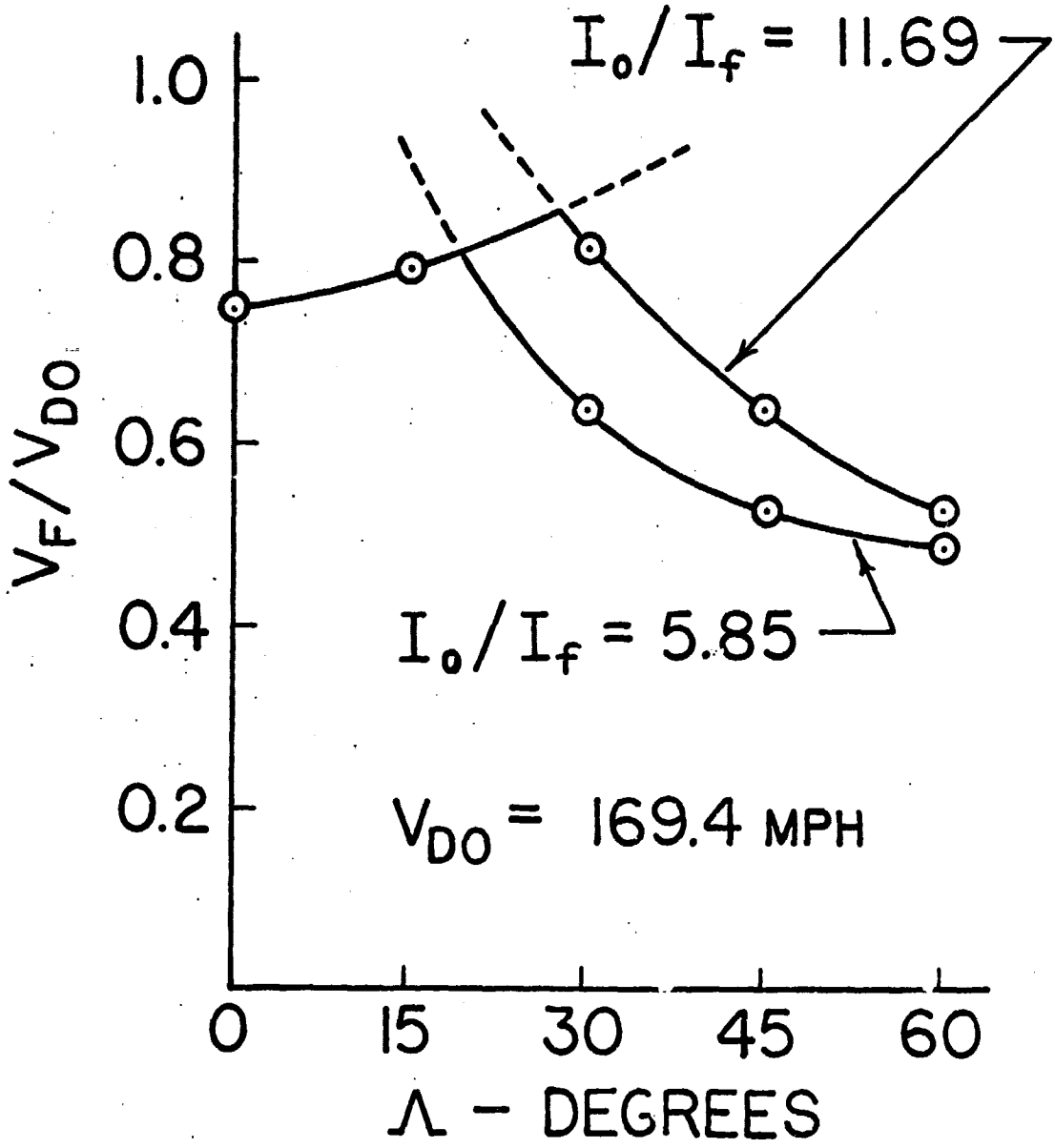

Fig. 5: Effect on flutter of doubling the fuselage moment of inertia in roll, I_f. (Ref. 8).

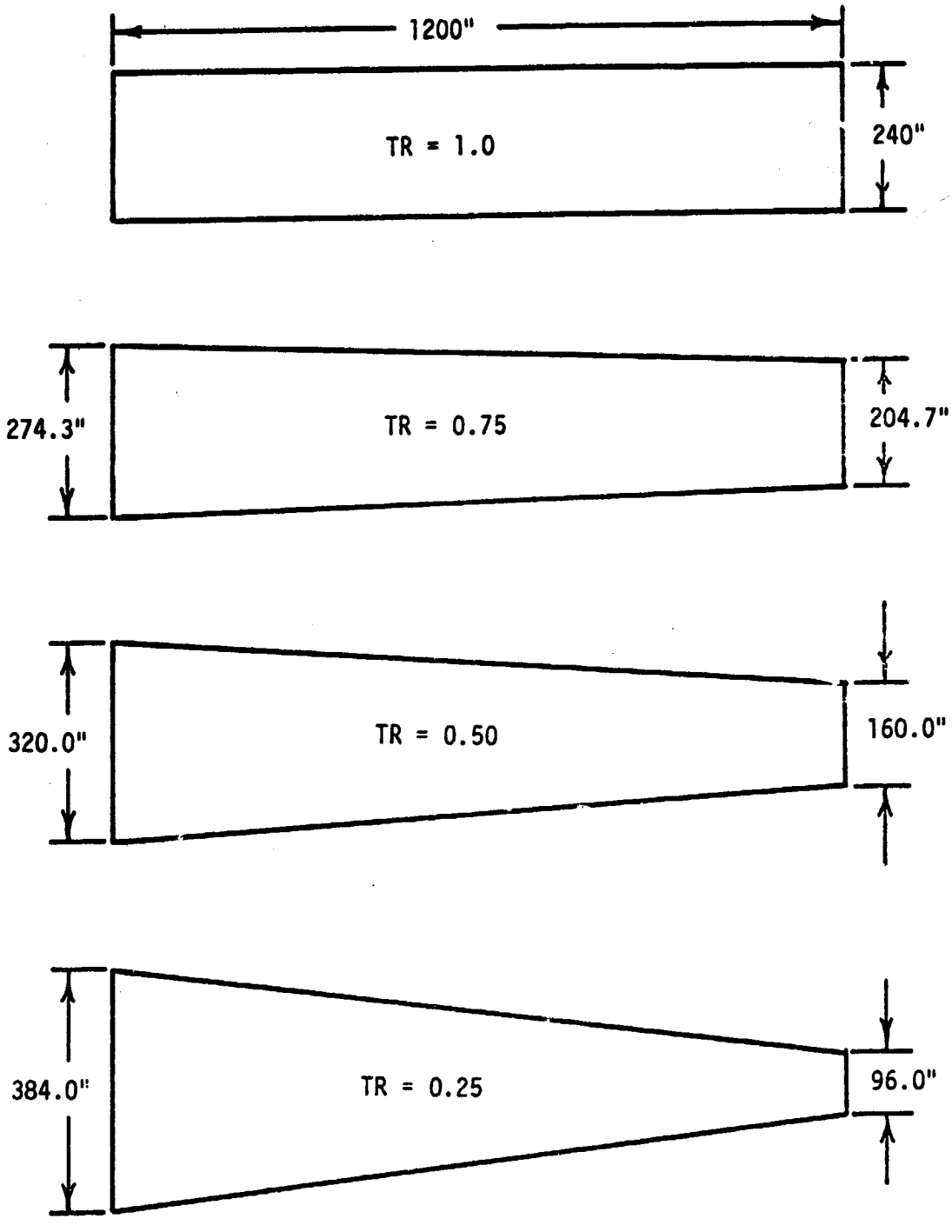

Fig. 6: Four semi-span planforms with differing taper ratio. (Ref. 6).

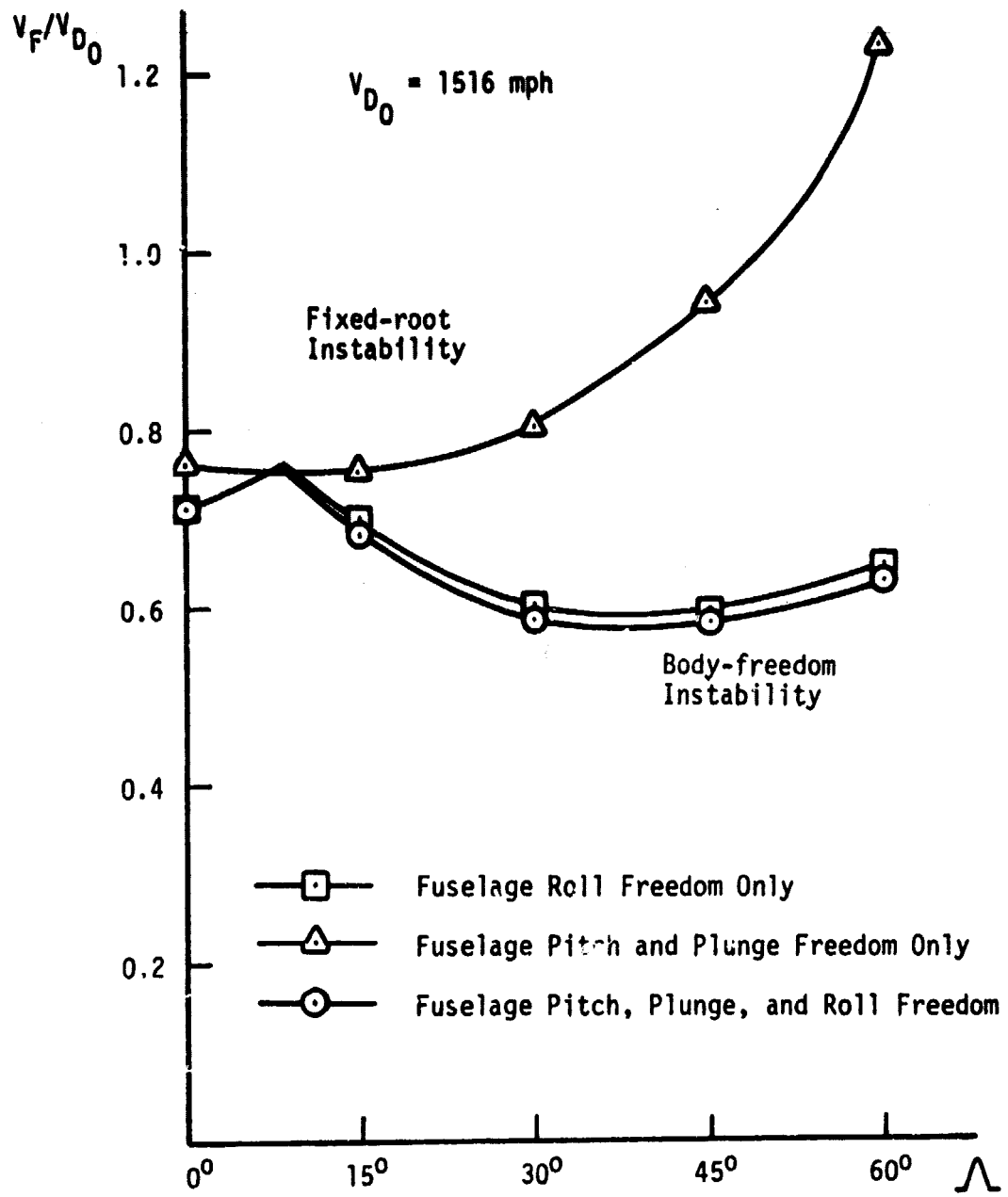

Fig. 7: Nondimensionalized Flutter Speeds, Based on the Inclusion of Rigid Body Plunge, Pitch, and Roll Degrees of Freedom, for the Full-size Planform with a Taper Ratio = 0.5; Incompressible Aerodynamics; Altitude-40,000 feet. (Ref. 6).

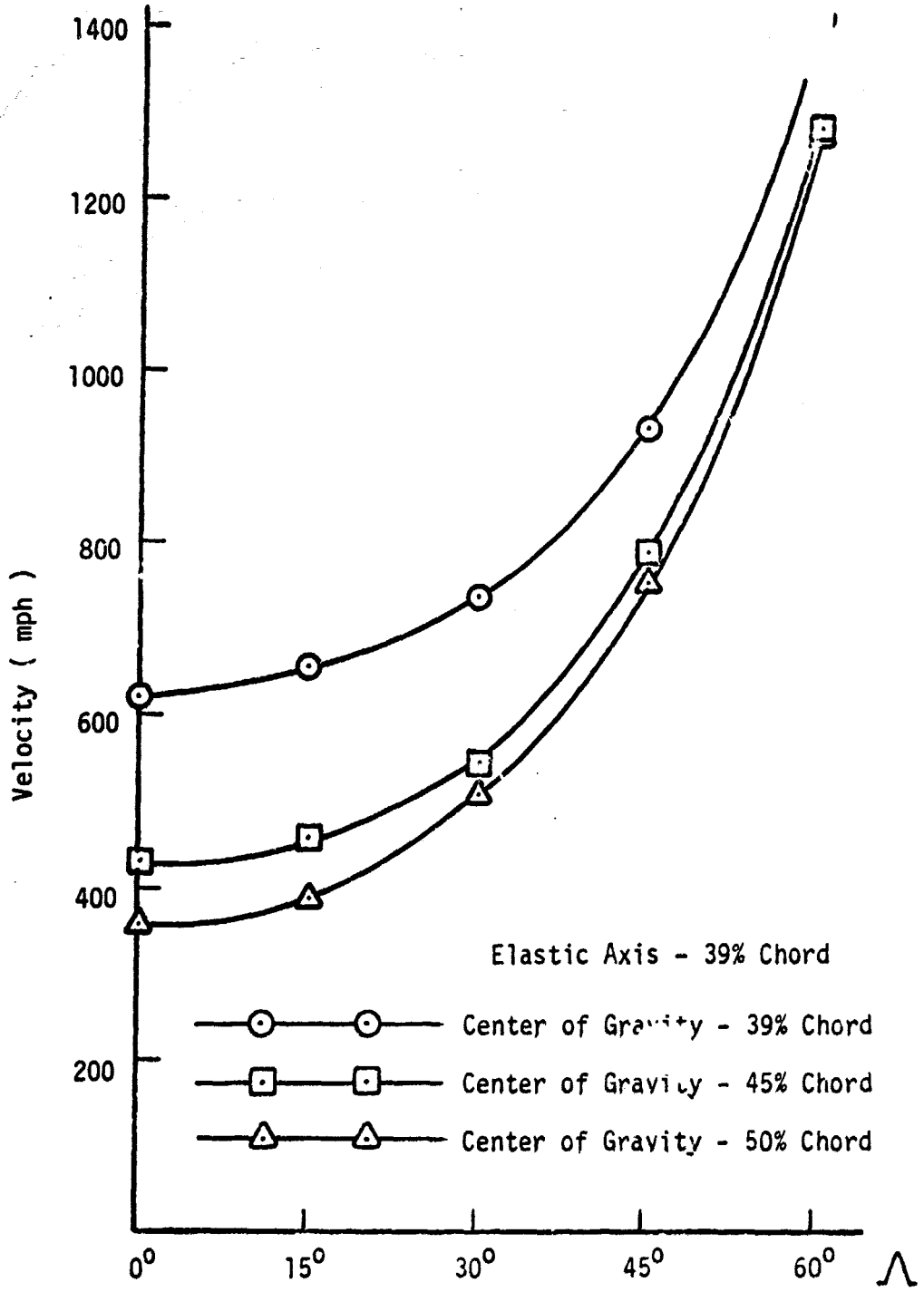

Fig. 8: The effect of wing center of gravity chordwise position on flutter speed. Wing with taper ratio 0.50. Incompressible aerodynamics at 40,000 ft. altitude. (Re 6).

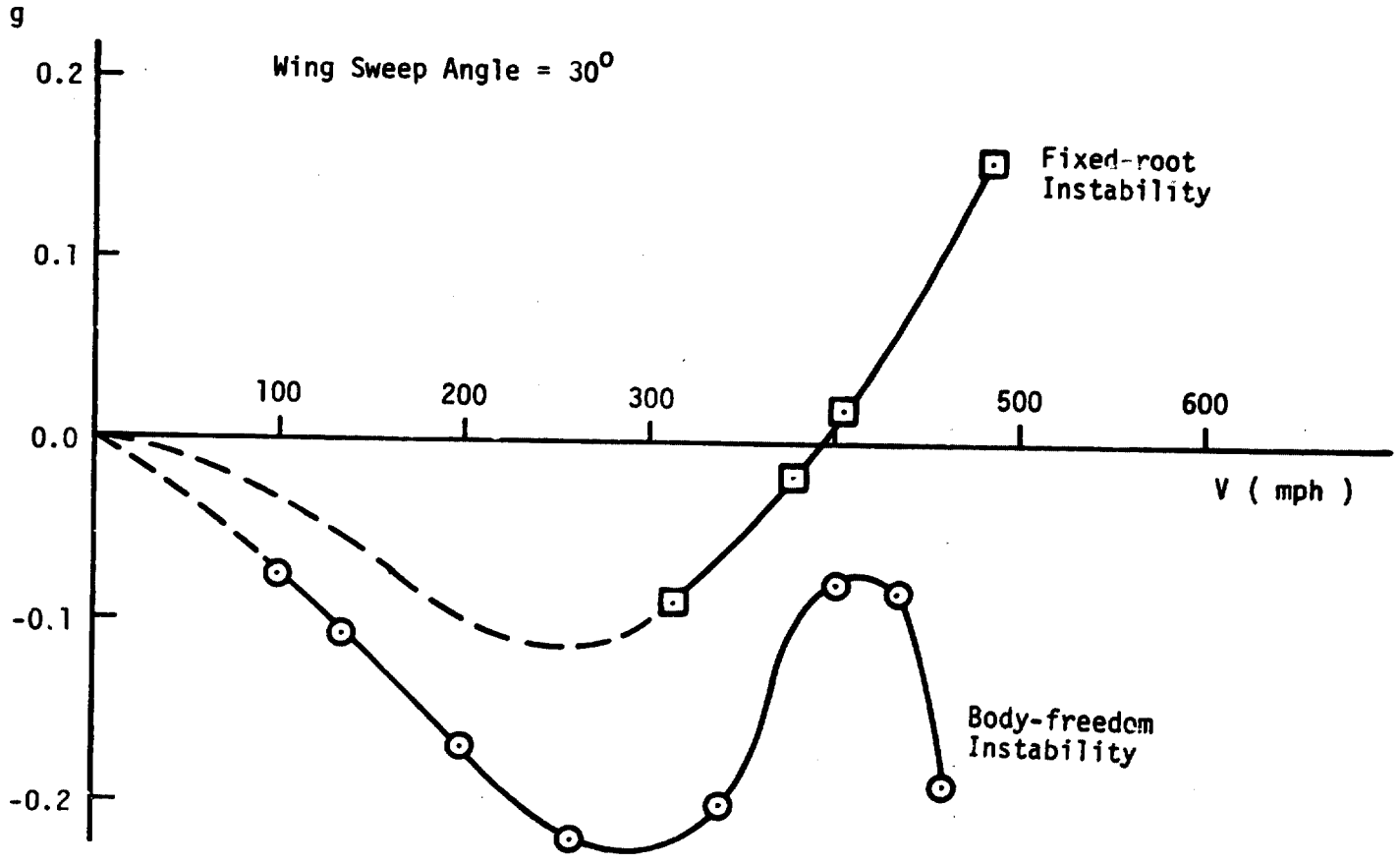

Fig. 9: The Effect of Sweep Angle on the Mode of Instability of the Full-size Planform with a Taper Ratio = 1.0; Incompressible Aerodynamics; Altitude-Sea Level. (Ref. 6).

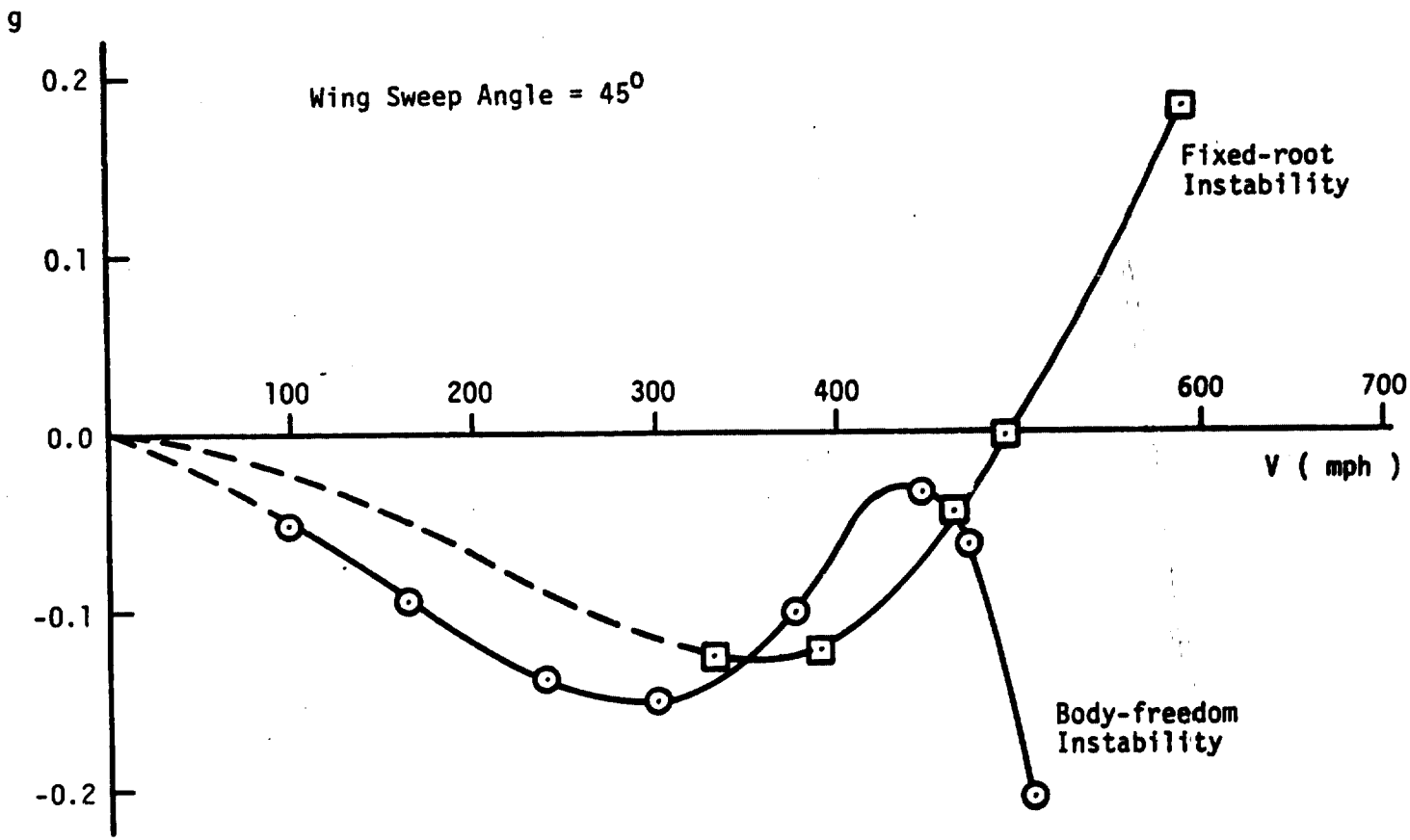

Fig. 10: The Effect of Sweep Angle on the Mode of Instability of the Full-size Planform with a Taper Ratio = 1.0; Incompressible Aerodynamics; Altitude-Sea Level. (Ref. 6).

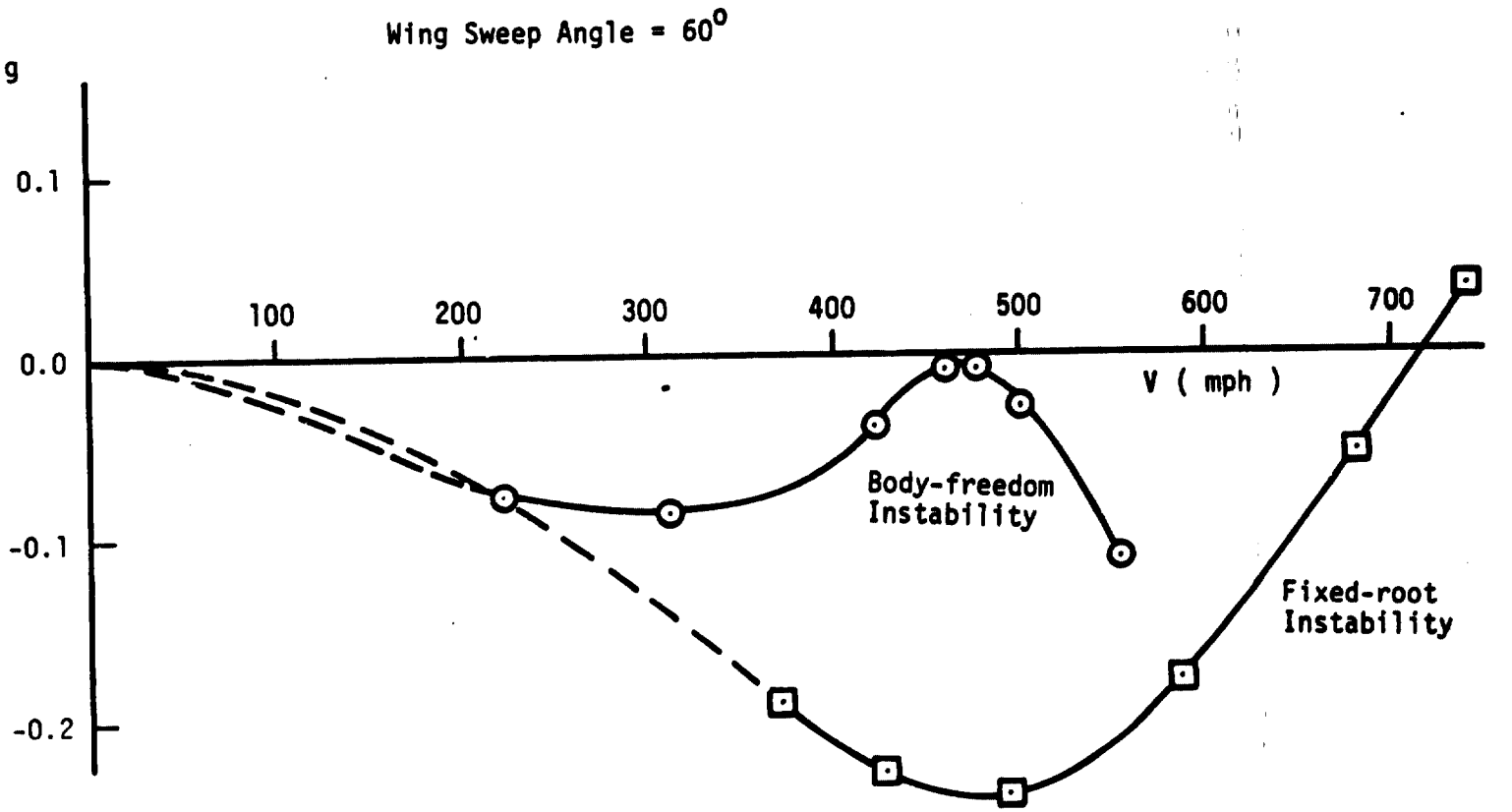

Fig. 11: The Effect of Sweep Angle on the Mode of Instability of the Full-size Planform with a Taper Ratio = 1.0; Incompressible Aerodynamics; Altitude-Sea Level. (Ref. 6).

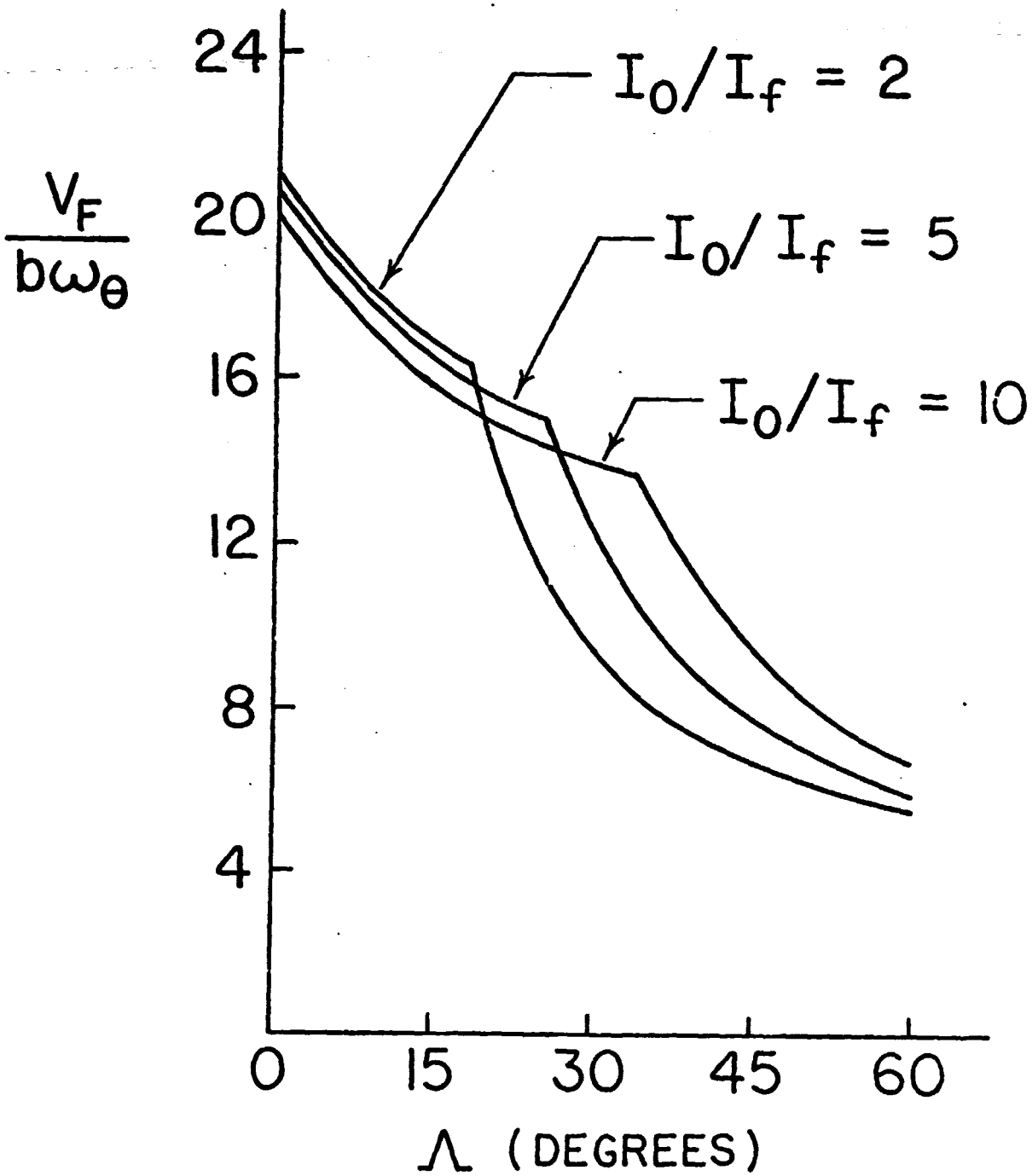

Fig. 12: The effect, on flutter, of the ratio of unswept wing mass moment of inertia in roll to fuselage mass moment of inertia in roll. Parameters are: $M = 2.5$, $\bar{AR} = 12.0$; $x_\theta = 0.10$; $r_\theta = 0.40$; $a = -0.10$; $\omega_B/\omega_\theta = 0.20$; $\mu = 50$. (Ref. 9).

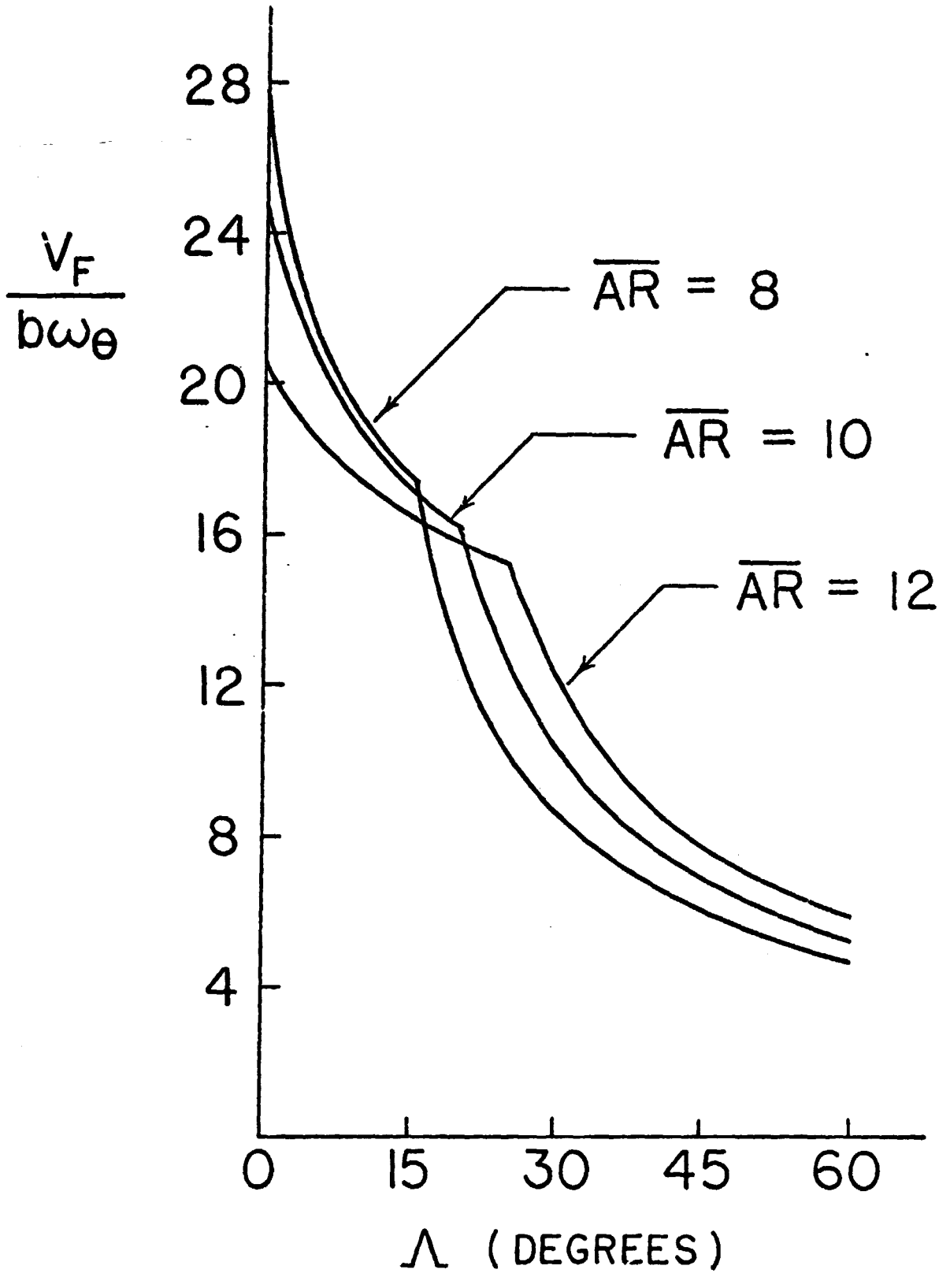

Fig. 13: The effect of aspect ratio, $\overline{AR}$, on flutter. Parameters are: M = 2.5; R = 5; x_θ = 0.10; r_θ = 0.40; a = -0.10; ω_B/ω_θ = 0.20; μ = 50. (Ref. 9).

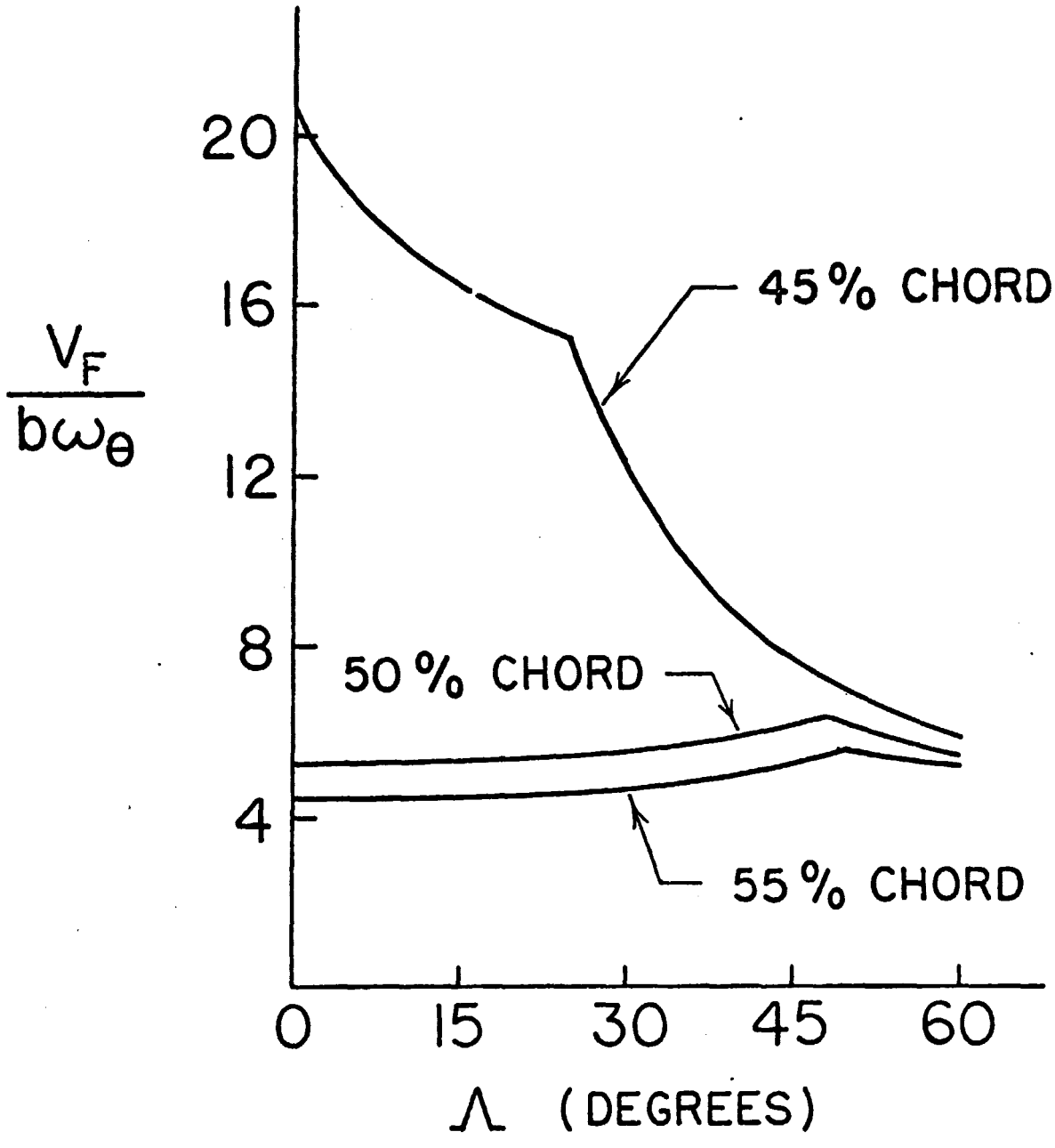

Fig. 14: The effect of elastic axis position on flutter. Parameters are: $M = 2.5$; $R = 5$; $\bar{AR} = 12$; $x_\theta = 0.10$; $r_\theta = 0.40$; $\mu = 50$; $\omega_B/\omega_\theta = 0.20$. (Ref. 9).

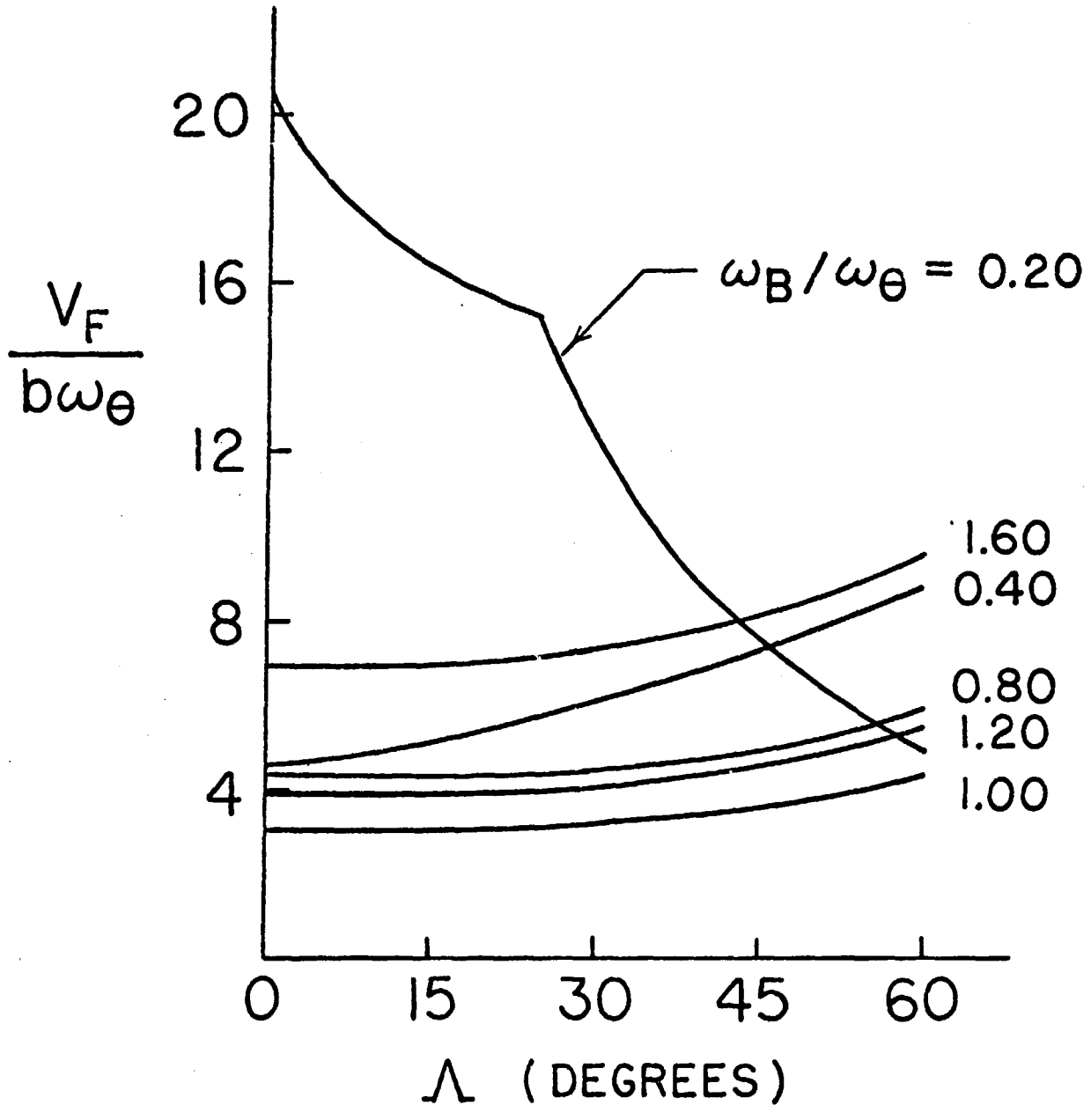

Fig. 15: The effect, on flutter, of the ratio of fundamental bending frequency to fundamental torsional frequency, ω_B/ω_θ. Frequencies are those of a clamped wing. Parameters are: M = 2.5; $\overline{AR}$ = 12; x_θ = 0.10; r_θ = 0.40; a = - 0.10; μ = 50. (Ref. 9).

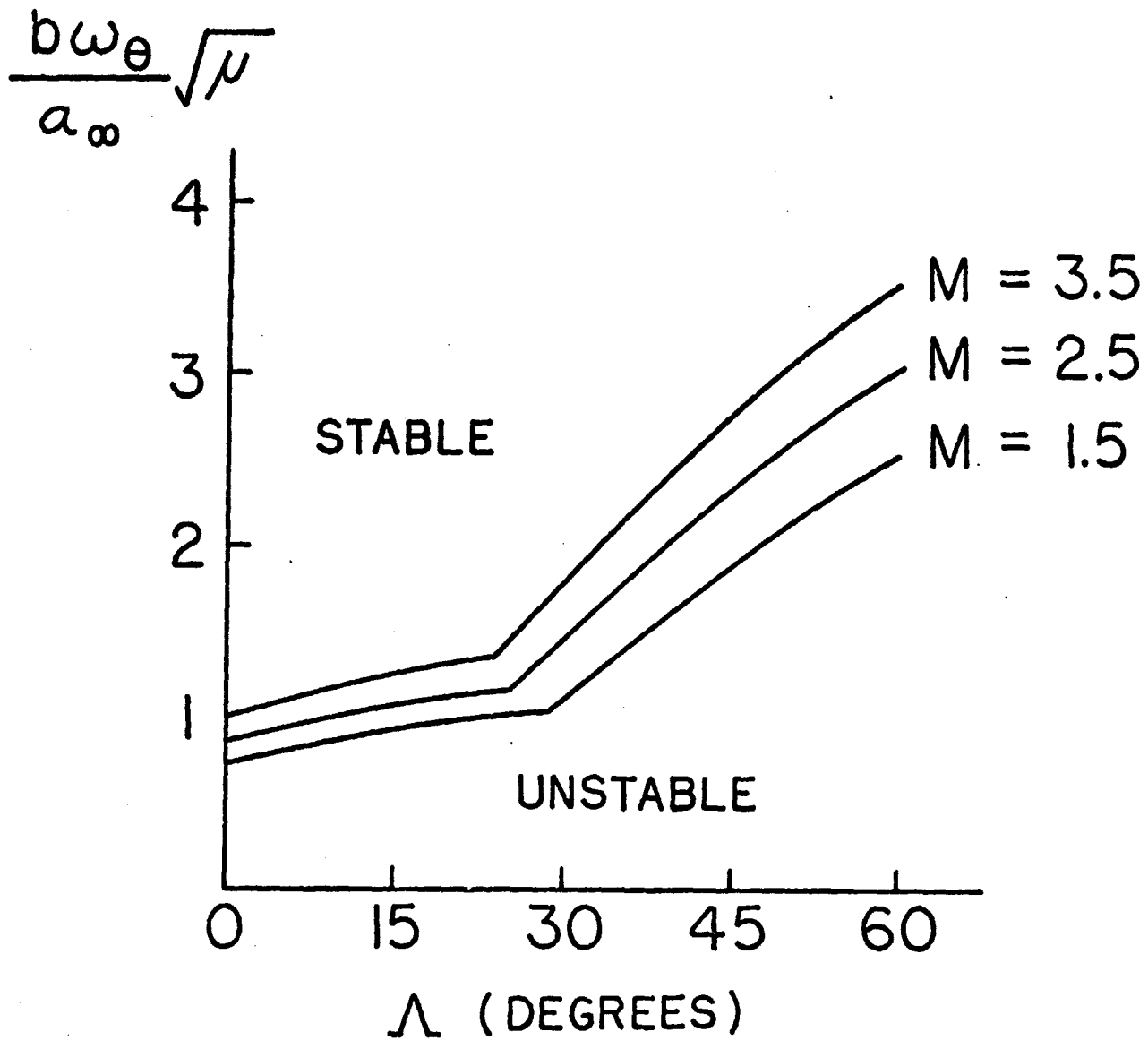

Fig. 16: The effect of Mach number on the stiffness-altitude parameter, β. Parameters are: $\bar{AR}$ = 12; x_θ = 0.10; r_θ = 0.40; a = - 0.10; ω_B/ω_θ = 0.20; μ = 50. (Ref. 9).

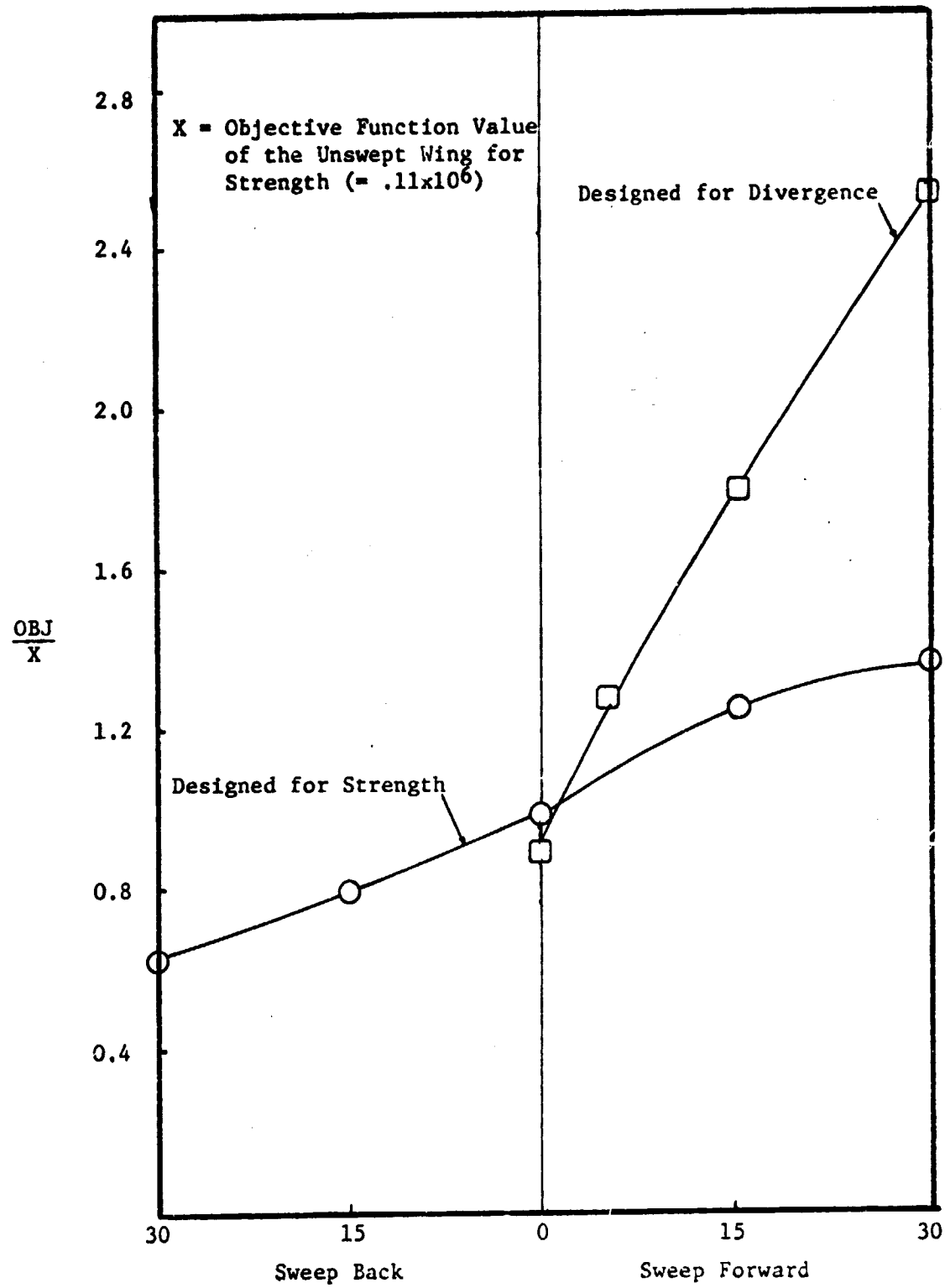

Fig. 17: Final relative weight of wing bending material with respect to an unswept, strength-designed wing. (Ref. 10).

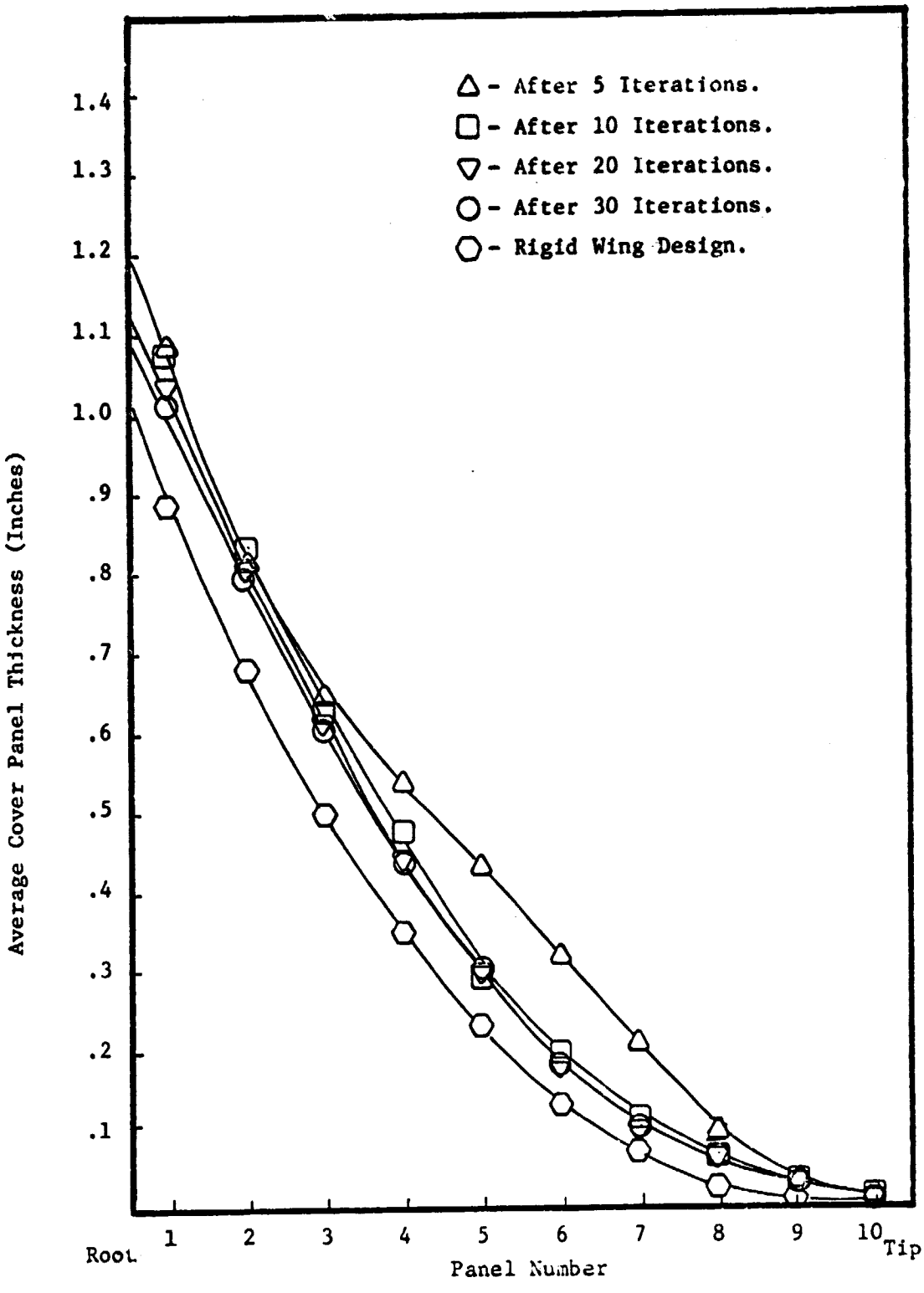

Fig. 18: Cover-sheet thickness distribution along the semi-span for a strength-designed unswept wing. (Ref. 10).

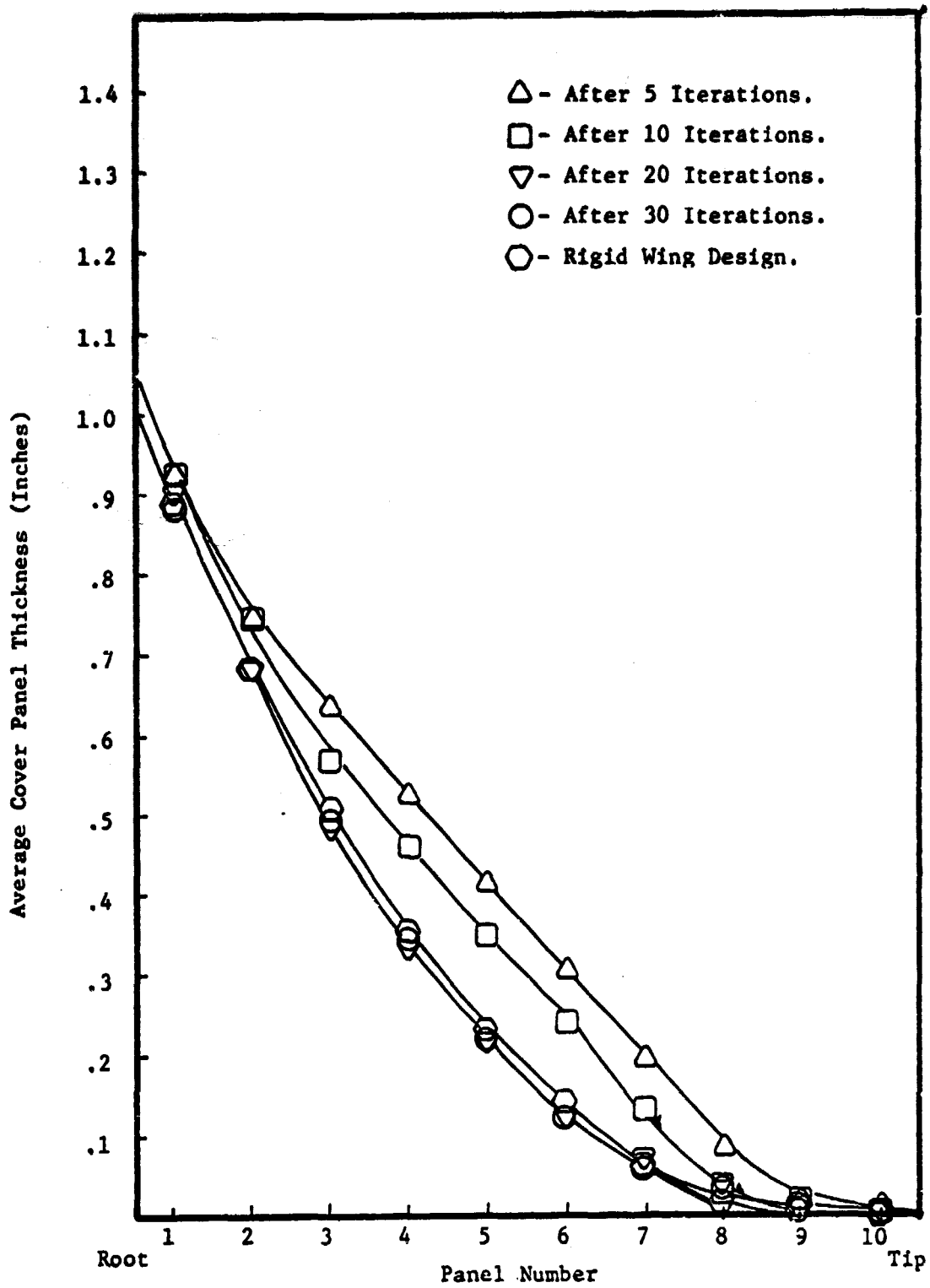

Fig. 19: Cover-sheet thickness distribution along the semi-span for a strength-designed 15 degree symmetrically sweptback wing. (Ref. 10).

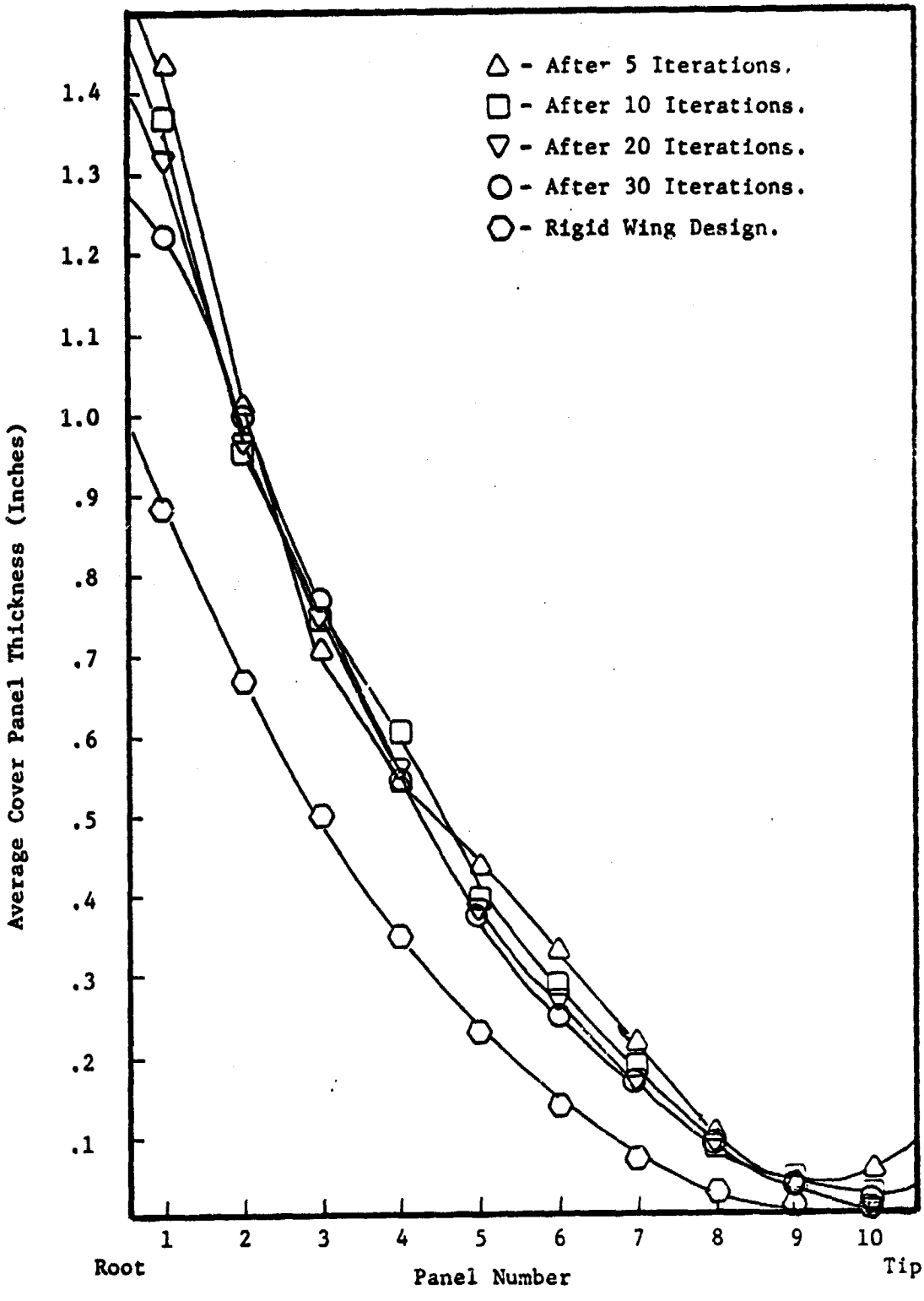

Fig. 20: Cover-sheet thickness distribution along the semi-span for a 15 degree symmetrically sweptforward wing. (Ref. 10).

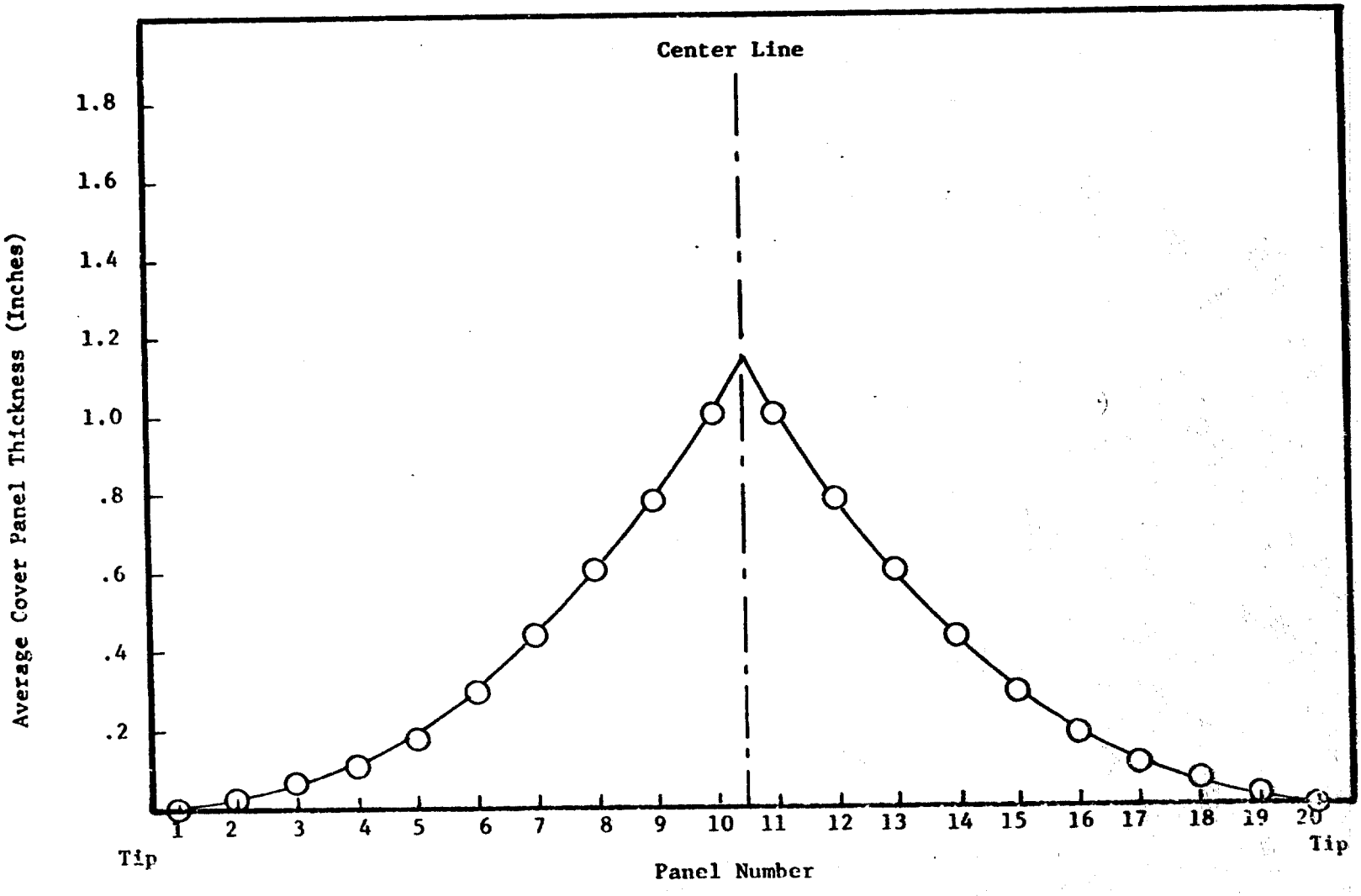

Fig. 21: Spanwise cover-sheet thickness distribution for an optimal unswept wing with strength and divergence constraints. (Ref. 10).

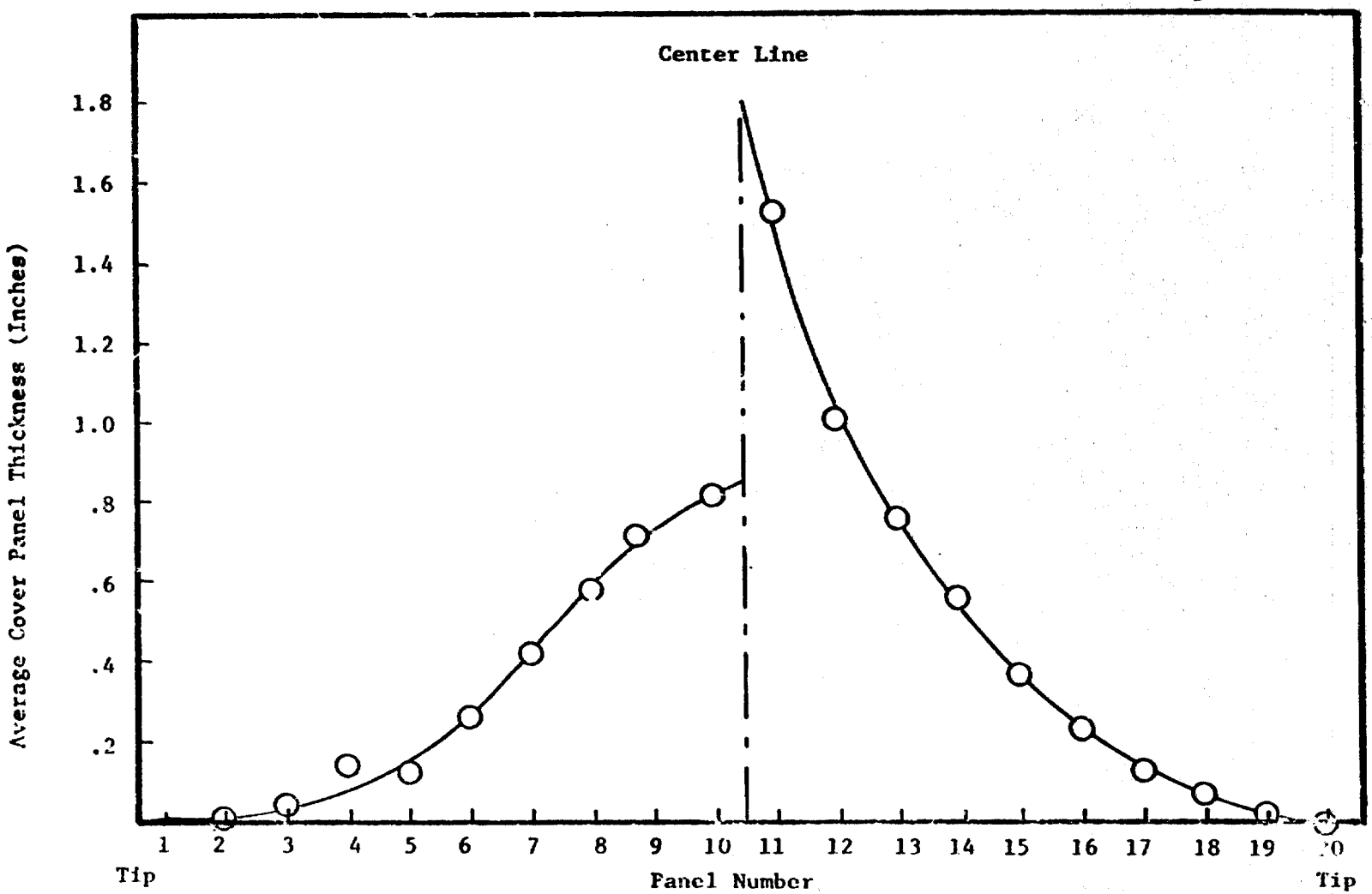

Fig. 22: Spanwise cover-sheet thickness distribution for an optimal 5 degree obliquely swept wing with strength and divergence constraints. (Ref. 10).

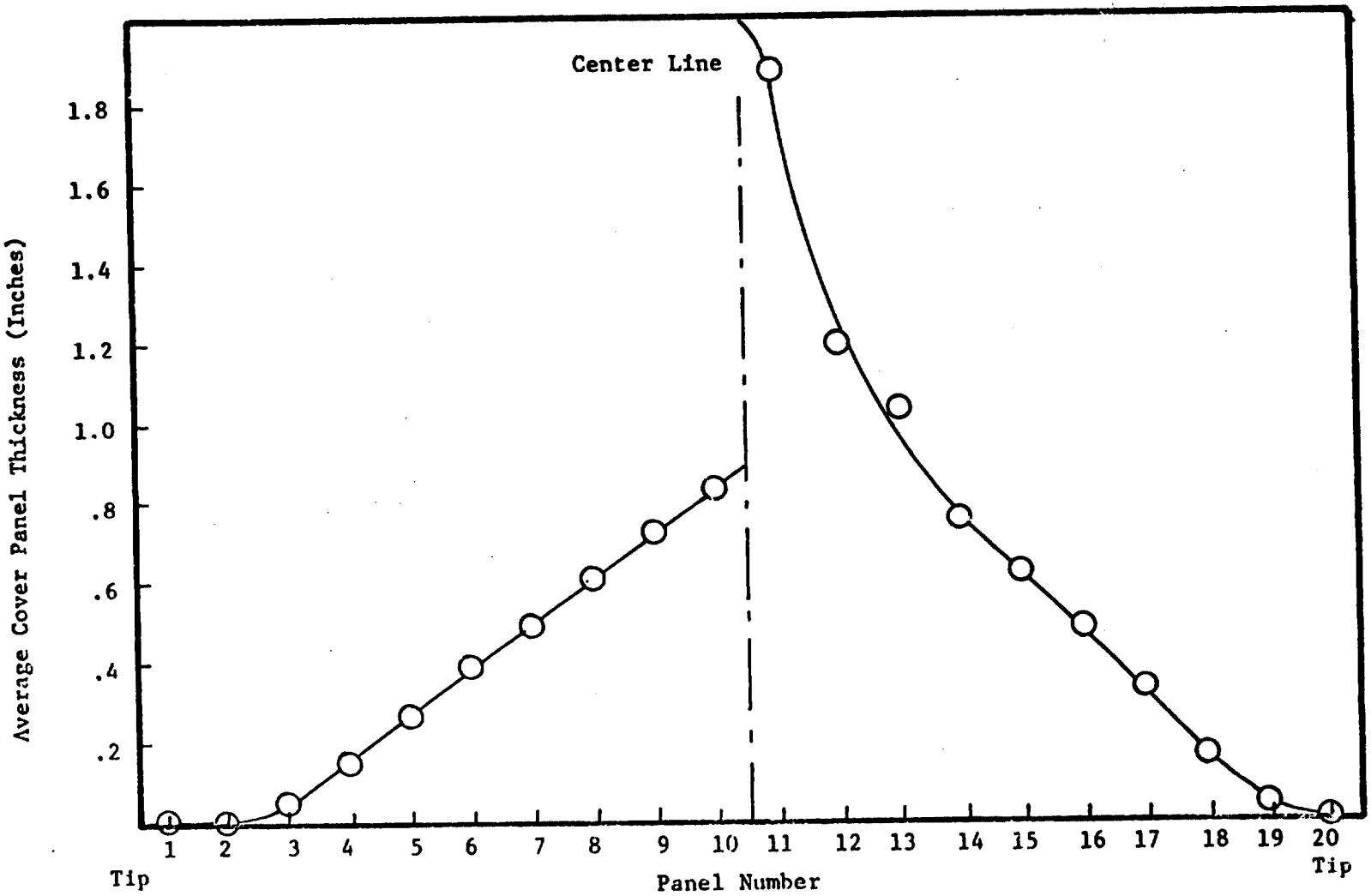

Fig. 23: Spanwise cover-sheet thickness distribution for an optimal 15 degree obliquely swept wing with strength and divergence constraints. (Ref. 10).

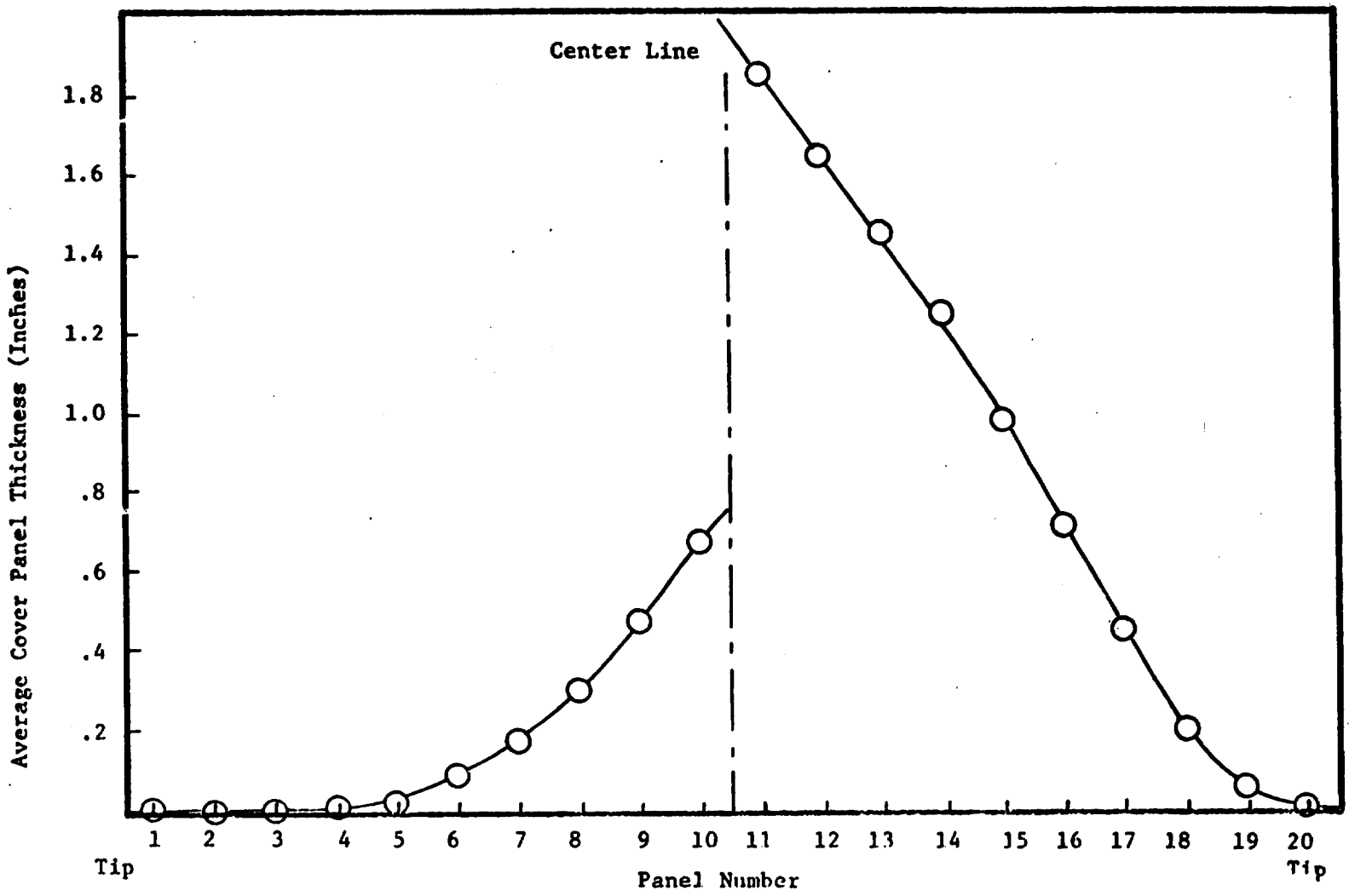

Fig. 24: Spanwise cover-sheet thickness distribution for an optimal 30 degree obliquely swept wing with strength and divergence constraints. (Ref. 10).

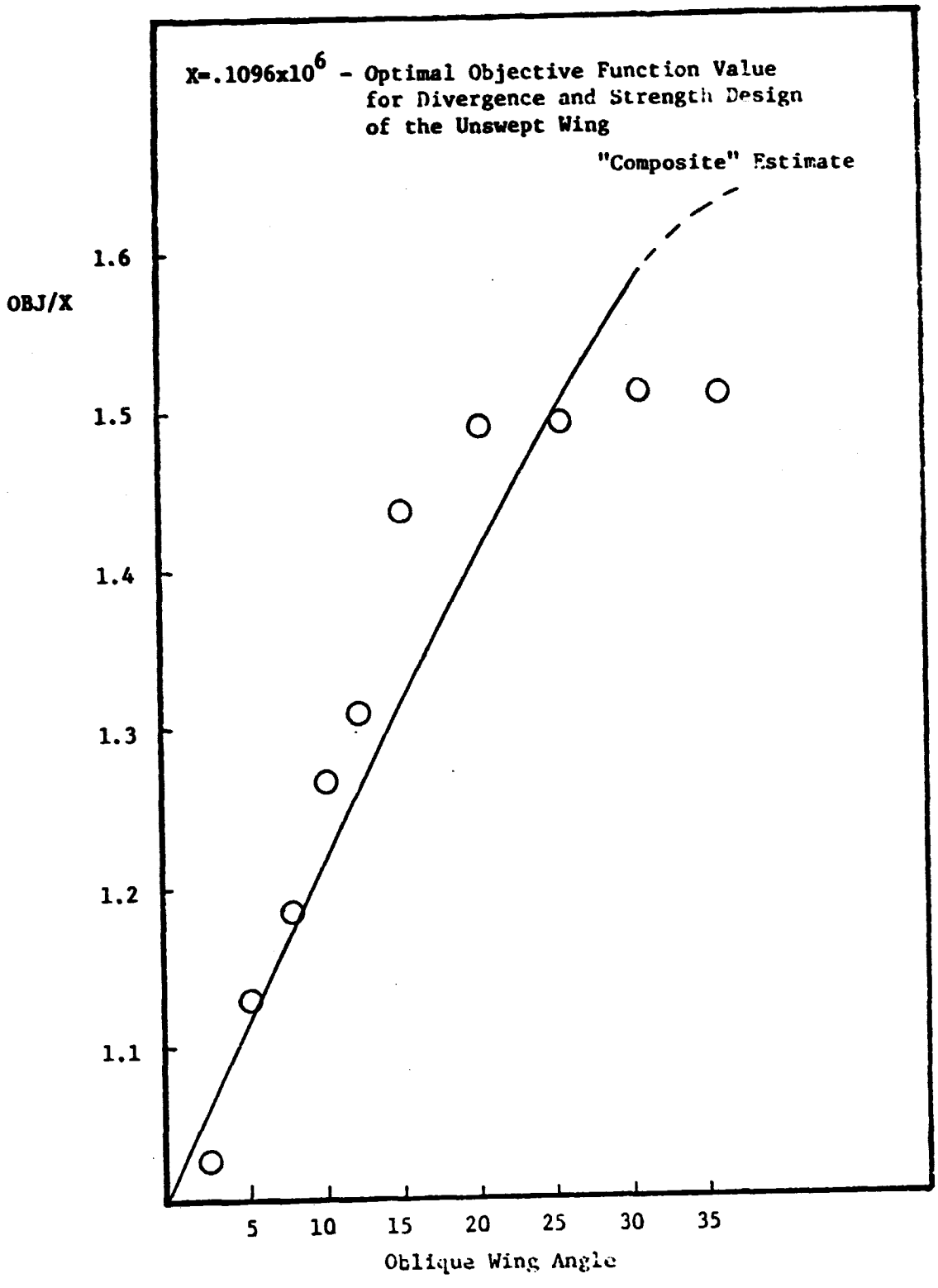

Fig. 25: Relative weights for obliquely swept wings with strength and divergence constraints. Unswept wing relative weight is equal to unity. (Ref. 10).